

# The bivalve *Glycymeris planicostalis* as a high-resolution paleoclimate archive for the Rupelian (Early Oligocene) of Central Europe

E. O. Walliser<sup>1</sup>, B. R. Schöne<sup>1</sup>, T. Tütken<sup>1</sup>, J. Zirkel<sup>1,\*</sup>, K. I. Grimm<sup>1</sup> and J. Pross<sup>2</sup>

[1]{Institute of Geosciences, University of Mainz, Johann-Joachim-Becher-Weg 21, 55128 Mainz, Germany}

[2]{Paleoenvironmental Dynamics Group, Institute of Earth Sciences, University of Heidelberg, Im Neuenheimer Feld 234, 69120 Heidelberg, Germany}

[\*]{now at: Institute of Geosciences, University of Frankfurt, Altenhöferallee 1, 60438 Frankfurt am Main, Germany}

Correspondence to: E. O. Walliser (walliser@uni-mainz.de)

## Abstract

Current global warming is likely to result in a unipolar glaciated world with unpredictable repercussions on atmospheric and oceanic circulation patterns. These changes are expected to affect seasonal extremes and the year-to-year variability of seasonality. To better constrain the mode and tempo of the anticipated changes, climatologists require ultra-high-resolution proxy data of time intervals in the past, e.g. the Oligocene, during which boundary conditions were similar to those predicted for the near future. In the present paper, we assess if such information can be obtained from shells of the long-lived bivalve mollusk *Glycymeris planicostalis* from the late Rupelian of the Mainz Basin, Germany. Our results indicate that the studied shells are pristinely preserved and provide an excellent archive to reconstruct changes of sea surface temperature on seasonal to inter-annual time scales. Shells of *G. planicostalis* grew uninterruptedly during winter and summer and therefore recorded the full seasonal temperature amplitude that prevailed in the Mainz Basin ~30 Ma ago. Absolute sea surface temperature data were reconstructed from  $\delta^{18}\text{O}_{\text{shell}}$  values assuming a  $\delta^{18}\text{O}_{\text{water}}$  signature that was extrapolated from coeval sirenian tooth enamel. Reconstructed values range between 12.3°C and 22.0°C and agree well with previous estimates based on planktonic foraminifera and shark teeth. However, temperatures during seasonal extremes vary greatly on inter-annual time scales. Mathematically re-sampled (i.e., corrected for uneven number of

1 samples per annual increment) winter and summer temperatures averaged over 40 annual  
2 increments of three specimens equal  $13.6 \pm 0.8^{\circ}\text{C}$  and  $17.3 \pm 1.2^{\circ}\text{C}$ , respectively. Such high-  
3 resolution paleoclimate information can be highly relevant for numerical climate studies  
4 aiming to predict possible future climates in a unipolar glaciated or, ultimately, polar ice-free  
5 world.

6

## 7 **1 Introduction**

8 Current  $\text{CO}_2$ -induced global warming is likely to result in a unipolar glaciated world  
9 ultimately followed by one without polar ice caps (e.g. Raper and Braithwaite, 2006). In light  
10 of these predicted boundary conditions, climate is expected to change profoundly, particularly  
11 at higher latitudes. According to numerical climate models, reduced meridional gradients will  
12 lead to substantial changes in atmospheric and oceanic circulation patterns (e.g., Cai & Chu,  
13 1998; Hansen et al., 2004), thereby affecting seasonality as well as the frequency and  
14 intensity of decadal climate oscillations (e.g. Marshall et al., 2001; Solomon et al., 2007). In  
15 turn, this will alter surface temperature patterns, storm intensities and precipitation rates  
16 (Hurrell, 1995; Dai et al., 1997; Barbosa, 2009), all of which present a major challenge to  
17 densely populated coastal areas and coastal ecosystems, particularly in Europe (Ottersen et al.,  
18 2001; Stenseth et al., 2002).

19 To date, the mode and tempo of the environmental change anticipated for the near future have  
20 remained poorly constrained (e.g., Vellinga and Wood, 2002; Hátún et al., 2005). This applies  
21 specifically to time scales of human perception, i.e., seasonal extremes and inter-annual  
22 variability. A promising avenue toward a better understanding of future climates is to  
23 investigate the short-term climate variability of time intervals in the past during which  
24 boundary conditions were similar to those predicted for the coming millennia. The last time a  
25 unipolar glaciated world occurred in Earth history was during the early Oligocene when  
26 atmospheric  $\text{CO}_2$  levels were slightly higher than today (Zachos et al., 2008) and the  
27 paleogeographic configuration on a global scale was at least broadly similar to the present-  
28 day situation (Lefebvre et al., 2013). Thus, the Oligocene world can serve as a natural  
29 laboratory for studying the possible effects of anthropogenic global warming. As yet,  
30 however, the Oligocene has remained a relatively poorly studied epoch of Earth history,  
31 which is at least partially attributed to the stratigraphic incompleteness of many Oligocene

1 successions. In particular, shallow-water sequences of Oligocene age are often compromised  
2 by unconformities resulting from strong, glacially induced eustatic sea-level fluctuations (e.g.,  
3 Miller et al., 2005; Pälke et al., 2006).

4 The epicontinental sedimentary archives from the Oligocene of Central Europe, notably the  
5 Rhenish triple junction system (e.g., Sissingh, 2003), can play a prime role in elucidating the  
6 short-term (i.e., seasonal to inter-annual) climate dynamics during that time. The significance  
7 of Oligocene sediments from the Rhenish triple junction system was first stressed by Beyrich  
8 (1854), whose work on strata from the Mainz and Kassel Basins ultimately led to the coinage  
9 of the term „Oligocene“. These shallow marine successions exhibit much higher  
10 sedimentation rates and generally contain more macrofossils than their open marine  
11 counterparts. Moreover, the shallow water depth and the low water-mass inertia as compared  
12 to the open ocean make them particularly sensitive to short-term paleoclimatic and  
13 paleoceanographic change. Furthermore, these strata contain well-preserved shells of long-  
14 lived bivalves (*Glycymeris planicostalis*, Lamarck 1819). Modern *Glycymeris* spp. have  
15 recently been identified as promising tools for ultra-high-resolution climate reconstructions  
16 (Brocas et al., 2013; Royer et al., 2013; Bušelić et al., 2014). This genus occurs worldwide in  
17 subtidal settings and lives infaunally in sandy and gravelly sediments (Ansell and Trueman,  
18 1967; Thomas, 1978). Their fossil history dates back to the Aptian (Gillet, 1924; Casey, 1961)  
19 and despite some evolutionary innovations acquired during the early Cenozoic, their  
20 fundamental *bauplan* has remained largely unvaried until today (Thomas, 1975).

21 Bivalve shells serve as reliable recorders of ambient environmental conditions (e.g.,  
22 Wanamaker et al., 2011). The production of shell material occurs on a periodic basis resulting  
23 in the formation of distinct growth lines that separate the growth pattern into time slices of  
24 equal duration, so-called growth increments. These growth patterns serve as a calendar which  
25 can be used to place each shell portion and each geochemical data point in a precise temporal  
26 context. Some bivalve species live for decades to several centuries and can therefore provide  
27 uninterrupted records of seasonality such as the genera *Glycymeris* (Ramsay et al., 2000;  
28 Brocas et al., 2013), *Arctica* (e.g. Ropes, 1985; Butler et al., 2013) and *Panopea* (e.g., Strom  
29 et al., 2004; Black et al., 2008).

30 In the present study, we have analyzed the ontogenetically young shell portions of three *G.*  
31 *planicostalis* specimens from the upper Rupelian of the Mainz Basin, SW Germany, with

1 regard to their oxygen isotopic composition in order to assess their potential as ‘deep-time’  
2 archives of paleoseasonality. Such data are currently not available. In particular, we focused  
3 on elucidating (i) whether the shells are sufficiently well preserved to permit reconstruction of  
4 water temperatures from shell oxygen isotope data; (ii) what the timing and rate of seasonal  
5 shell growth of these specimens were; and (iii) how the seasonal  $\delta^{18}\text{O}_{\text{shell}}$ -derived water  
6 temperatures compare to existing temperature proxy data from that region. In order to assess  
7 the oxygen isotope composition of the local seawater ( $\delta^{18}\text{O}_{\text{water}}$ ) in the Mainz Basin during the  
8 Rupelian we measured the phosphate oxygen isotope composition ( $\delta^{18}\text{O}_{\text{PO}_4}$ ) of the enamel of  
9 seven teeth of the sea cow *Halitherium schinzii* from the same formation as the *G.*  
10 *planicostalis* shells. The  $\delta^{18}\text{O}_{\text{PO}_4}$  value has been successfully exploited as a  $\delta^{18}\text{O}_{\text{water}}$  proxy by  
11 many authors (e.g. Clementz and Koch, 2001, Clementz et al., 2006, Thewissen et al., 2007  
12 and Clementz and Sewall, 2009). Hence, this study lays the groundwork for future ultra-high  
13 resolution paleoclimate reconstructions for the Oligocene.

14

## 15 **2 Material and methods**

### 16 **2.1 Study area**

17 The Mainz Basin is located near the northwestern margin of the Upper Rhine Graben. Its  
18 formation dates back to the middle Eocene and is related to the taphrogenesis of the European  
19 Cenozoic rift system (Dèzes et al., 2004; Ritzkowski, 2005; Grimm et al., 2011) (Fig. 1). Its  
20 sedimentary succession, which was mainly deposited in shallow marine and brackish settings,  
21 covers a time interval of ca. 20 Ma, from the Lutetian (~49.5 Ma) to the early Burdigalian  
22 (~18.5 Ma). During the late Rupelian (i.e., late Early Oligocene; 34.9 – 28.4 Ma; Gradstein et  
23 al., 2004), central Europe experienced a period of extended marine transgressions due to local  
24 tectonic subsidence and eustatic sea level rise. As a consequence, the Mainz Basin became  
25 part of a marine strait that extended from the paleo-North Sea Basin to the southernmost  
26 Upper Rhine Graben (Picot, 2002; Sissingh, 2003; Berger et al., 2005a). A possible southern  
27 connection with the western Molasse Basin has been controversially debated (Martini, 1982;  
28 Picot, 2002; Berger et al., 2005a, 2005b; Grimm, 2006).

29 According to Berger et al. (2005b), marine conditions in the Mainz Basin lasted for about 2.5  
30 Ma from the sea-level high stand Ru2/Ru3 (~32 Ma) to Ru3/Ru4 (~29.5 Ma) of Haq et al.

1 (1988). Nearshore deposits representing that time comprise coarse-grained (sand to gravel)  
2 siliciclastics of the Alzey Formation (from which the studied fossil material was collected –  
3 see below) and the overlaying Stackeden Formation. Contemporaneously deposited basal  
4 sediments (pelites) belong to the Bodenheim Formation (Grimm et al., 2000; Sissingh, 2003;  
5 Berger et al., 2005b). Age control for the marine strata of the Mainz Basin is mainly based on  
6 calcareous nanoplankton (Martini and Müller, 1971; Martini, 1982), dinoflagellate cysts (e.g.,  
7 Pross, 1997), and, to a lesser extent, benthic foraminifera (Grimm, 1998, 2002). With regard  
8 to the nanoplankton zonation, the Alzey and Bodenheim Formations comprise the upper part  
9 of nanoplankton zone NP23 and the lower part of nanoplankton zone NP24 (Grimm, 1994;  
10 Pross and Schmiedl, 2002; Berger et al., 2005b).

11 Paleoenvironmental reconstructions of the Alzey Formation are based on palynological and  
12 faunal data indicating an overall warm climate comparable to modern subtropical climate  
13 zones of the Mediterranean (Grimm et al., 2011). Reconstructed mean annual air temperature  
14 in the hinterland fluctuated between  $\sim 16^{\circ}$  and  $\sim 17^{\circ}\text{C}$ , and mean annual precipitation was  
15 between 1000 and 1250 mm per year (Pross et al., 1998; Pross et al., 2000). The Mainz Basin  
16 experienced repeated alternations between drier and wetter conditions during the deposition of  
17 the Alzey Formation, which caused fluctuations in surface water salinity levels (remaining  
18 within the range of normal marine conditions) and the episodic formation of water-mass  
19 stratifications (Pross 2001; Pross and Schmiedl, 2002). Temperature estimates of the seawater  
20 have been derived from the  $\delta^{18}\text{O}$  values of shark teeth and foraminiferan tests. These  
21 estimates yielded values of  $6.9^{\circ}$  to  $23.3^{\circ}\text{C}$  for shallow-water settings (Tütken, 2003) and  $5.9^{\circ}$   
22 to  $14.9^{\circ}\text{C}$  for bottom waters (maximum depth: 150 m; Grimm, 1994; Grimm et al., 2011).

23

## 24 **2.2 Material**

25 The studied shell material was collected by Prof. Jürgen Boy during the 1970s and 1980s and  
26 has been stored at the Paleontological collection of the Institute of Geosciences in Mainz.  
27 Samples originate from the outcrop ‘Trift’ near Weinheim, the stratotype of the Alzey  
28 Formation (Grimm et al., 2000) (Fig. 1). Additional information about the precise  
29 stratigraphic position of the sampled layer is not available. The outcrop is  $\sim 8$  m thick and  $\sim 40$   
30 m wide; it consists of fossiliferous middle to coarse sands and fine gravels. Numerical dating  
31 with strontium isotope ( $^{87}\text{Sr}/^{86}\text{Sr}$ ) stratigraphy of a well-preserved bivalve shell from the

1 outcrop yielded an age of  $30.1 \pm 0.1$  Ma (Grimm et al., 2003). The outcrop exhibits a highly  
2 diverse and fully marine benthic fauna dominated by bivalves, gastropods and scaphopods  
3 that dwelled in shallow subtidal waters. Furthermore, corals were found suggesting limited  
4 seasonal salinity changes. Water-depth estimates, which are based on sedimentological  
5 features (Grimm et al., 2003) and ichnofossils (Schindler et al., 2005), range from ~30 to ~40  
6 m. The sea cow teeth originated from four localities located along the southwestern paleo-  
7 coastline of the Mainz Basin (Fig. 1; Table 1), and were stored at the Paleontological  
8 collection of the Institute of Geosciences and the collection of the Museum of Natural History  
9 Mainz (in german: Landessammlung für Naturkunde Rheinland-Pfalz)

10

### 11 **2.3 Methods**

12 From the *Glycymeris planicostalis* specimens collected at the outcrop “Trift”, three large  
13 valves (~8 cm in height) that visually appeared well-preserved were selected for further  
14 investigations. These valves were labeled (MB-Wht-2, MB-Wht-4 and MB-Wht-7), mounted  
15 on Plexiglas cubes with GlueTec Multipower plastic welder and coated with WIKO metal  
16 epoxy resin to avoid fracture during cross-sectioning. From each valve, two ca. 3 mm-thick  
17 slabs were cut perpendicular to the growth lines and along the axis of maximum growth from  
18 the umbo to the commissure using a low-speed precision saw (Buehler Isomet 1000; at 200  
19 rpm) equipped with a wafering-thin (0.4 mm), diamond coated blade. Both shell slabs were  
20 glued to glass slides with the mirroring sides facing up, ground on glass plates (320, 800,  
21 1200 grit SiC powder) and polished with 1  $\mu\text{m}$   $\text{Al}_2\text{O}_3$  powder. After each preparation step, the  
22 samples were ultrasonically rinsed in deionized water.

23 One polished slab of each specimen was firstly used for diagenetic screening. For this  
24 purpose, a set of different methods was employed including cathodoluminescence  
25 petrography, Raman spectroscopy and immersion of the shell slabs in Feigl solution. The  
26 presence of  $\text{Mn}^{2+}$  (>10-20 ppm) in calcium carbonates produces an orange  
27 cathodoluminescence (Machel et al., 1991) and is typically regarded as an indicator of  
28 diagenetic neomorphism (Grossman et al., 1996; Flügel, 2004) because biogenic aragonite is  
29 non-cathodoluminescent (Major, 1991). Like modern *Glycymeris* spp., shells of fossil  
30 representatives of this genus consisted of aragonite, which is prone to change to calcite during  
31 diagenesis. Raman spectroscopy can yield detailed and spatially highly resolved information

1 on the type of polymorphs of CaCO<sub>3</sub>. Likewise, the Feigl test can distinguish between  
2 aragonite and calcite (Feigl, 1958). Feigl solution stains aragonite black and calcite pale grey.  
3 After diagenesis screening, the shell slabs were ground and polished again, and prepared for  
4 sclerochronological studies and subsequent scanning electron microscopic (SEM) analyses.  
5 For this purpose, polished cross-sections were immersed in Mutvei's solution for 40 min  
6 under constant stirring at 37-40°C (Schöne et al., 2005a). After the staining process, the  
7 samples were gently rinsed in deionized water, air-dried and then photographed with a digital  
8 camera (Canon EOS 600D) mounted to a binocular microscope (Wild Heerbrugg M8).  
9 Growth increments were counted and their width measured with the image processing  
10 software Panopea (© Peinl & Schöne). Subsequently, samples were sputter-coated with a 2  
11 nm thick gold layer and viewed under a scanning electron microscope (LOT Quantum Design  
12 Phenom Pro, 2<sup>nd</sup> generation) in order to describe the prevailing microstructures and identify  
13 possible neomorphic minerals that may have formed during diagenesis (Fig. 2).

14 The other polished slab of each specimen was used for the analysis of oxygen isotope values  
15 ( $\delta^{18}\text{O}_{\text{shell}}$ ). Prior to the analysis, the outer ca. 0.5 to 1 mm thick chalky rim of the shell surfaces  
16 was physically removed (Fig. 2A-C). Then, 675 individual carbonate powder samples were  
17 micromilled from the outer shell layer (ventral margin) of the three specimens (316, 193 and  
18 166 samples from specimens MB-Wht-2, MB-Wht-4 and MB-Wht-7, respectively) using a  
19 Rexim Minimo dental drill mounted to a stereomicroscope and equipped with a cylindrical,  
20 diamond-coated bit (1 mm diameter; Komet/Gebr. Brasseler GmbH & Co. KG, model no. 835  
21 104 010). Sampling was performed in the ontogenetically youngest part of the shells.  
22 Individual milling steps contoured the shell growth patterns and measured between 100 and  
23 200  $\mu\text{m}$  in width. Carbonate powder samples weighing between 50 and 120  $\mu\text{g}$  were reacted  
24 with 100% phosphoric acid in He-flushed borosilicate exetainers at 72°C. The resulting CO<sub>2</sub>  
25 was measured with a GasBench II-coupled Thermo Finnigan MAT 253 gas source isotope  
26 ratio mass spectrometer in continuous flow mode at the Institute of Geosciences of the  
27 University of Mainz. Oxygen isotope values are reported in  $\delta$ -notation and given as parts per  
28 mil (‰). Data were calibrated against a NBS-19 calibrated IVA Carrara marble ( $\delta^{18}\text{O} = -1.91$   
29 ‰). On average, replicated internal precision ( $1\sigma$ ) and accuracy ( $1\sigma$ ) were better than 0.05‰,  
30 respectively.

31 If the bivalves formed their shell in oxygen isotopic equilibrium with the ambient water, the  
32  $\delta^{18}\text{O}_{\text{shell}}$  values can provide information on water temperature during growth (Epstein et al.,

1 1953). For aragonitic shells, the paleothermometry equation of Grossman and Ku (1986) with  
2 a scale correction of -0.27‰ (see Dettman et al., 1999) is typically employed:

$$3 \quad T_{\delta^{18}\text{O}} (\text{°C}) = 20.60 - 4.34 \cdot (\delta^{18}\text{O}_{\text{shell}} - (\delta^{18}\text{O}_{\text{water}} - 0.27)) \quad (1)$$

4 where  $\delta^{18}\text{O}_{\text{shell}}$  is measured relative to VPDB and  $\delta^{18}\text{O}_{\text{water}}$  relative to VSMOW. To compute  
5 reliable temperatures from  $\delta^{18}\text{O}_{\text{shell}}$  values also requires knowledge of the  $\delta^{18}\text{O}_{\text{water}}$  value  
6 during shell formation. This value was reconstructed from  $\delta^{18}\text{O}_{\text{PO}_4}$  values of tooth enamel of  
7 sea cows, i.e., homoeothermic marine mammals, from the same stratigraphic level. The  
8 average  $T_{\delta^{18}\text{O}}$  error was calculated by combining the average precision errors of the mass  
9 spectrometric analyses of bivalve shells and sirenian teeth (error propagation method). This  
10 resulted in an average  $T_{\delta^{18}\text{O}}$  error of  $\pm 0.4$  °C. An additional source of uncertainty is  
11 represented by the standard deviation of the reconstructed average  $\delta^{18}\text{O}_{\text{water}}$  values ( $\pm 0.3\text{‰}$ ).  
12 The integration of both values results in a combined temperature error of  $\pm 1.3$ °C.

13

#### 14 **2.4 Sea cow teeth**

15 The oxygen isotope composition of tooth enamel from marine vertebrates can provide  
16 information on the  $\delta^{18}\text{O}_{\text{water}}$  value of ambient seawater (e.g. Lécuyer et al., 1996; Clementz  
17 and Koch, 2001; Clementz et al., 2006; Clementz and Sewall, 2009). Therefore, we measured  
18 the phosphate oxygen isotope composition ( $\delta^{18}\text{O}_{\text{PO}_4}$ ) of the enamel from seven sirenian teeth  
19 of *Halitherium schinzii* recovered from the deposits of the Alzey Formation.

20 The surface of the teeth was physically cleaned and then sampled with a hand-held dental  
21 drill. Five teeth, which were large enough, were sampled twice, one sample at top and another  
22 one at the bottom of the crown. A fraction of each enamel powder sample was then treated  
23 with 2% NaOCl and 0.18 mL of 0.1 molar acetic acid to remove organics and potential  
24 diagenetic carbonates, respectively. Subsequently, ca. 4 mg of each pretreated sample were  
25 converted into silver phosphate ( $\text{Ag}_3\text{PO}_4$ ) following the method of O'Neil et al. (1994) with  
26 modifications of Dettman et al. (2001) and Tütken et al. (2006). Triplicates of 500 µg of each  
27  $\text{Ag}_3\text{PO}_4$  sample were analyzed with a Thermo Fisher Delta Plus XL mass spectrometer  
28 coupled to a TC-EA, at the University of Tübingen, Germany. Measured values were  
29 normalized to calibrated in-house standards, Tu-1 and Tu-2 (Vennemann et al., 2002) and  
30 reported in  $\delta$ -notation versus VSMOW. Replicate (n=6) analyses of NBS 120c (pretreated as



1 the samples) yielded a  $\delta^{18}\text{O}_{\text{PO}_4}$  value of  $21.6 \pm 0.13\text{‰}$  which agrees well with the value of  
2  $21.7\text{‰}$  reported by Lécuyer et al. (1993) and subsequently confirmed by many other  
3 laboratories (summarized in the appendix of Chenery et al., 2010). The  $\delta^{18}\text{O}_{\text{PO}_4}$  values of the  
4 *H. schinzii* teeth of the Mainz Basin were converted into  $\delta^{18}\text{O}_{\text{water}}$  values using the equation  
5 determined for modern sirenians by Tütken (2003):

$$6 \quad \delta^{18}\text{O}_{\text{water}} = \frac{\delta^{18}\text{O}_{\text{PO}_4} - 20.23}{0.86} \quad (2)$$

7

8 where  $\delta^{18}\text{O}_{\text{water}}$  and  $\delta^{18}\text{O}_{\text{PO}_4}$  are given relative to VSMOW. We used the equation of Tütken  
9 (2003) instead the one proposed by Lécuyer et al. (1996), because the calibration of Eq. 2 is  
10 based on more sea cow specimens and covers a 3-times larger range of measured ambient  
11  $\delta^{18}\text{O}_{\text{water}}$  values. However,  $\delta^{18}\text{O}_{\text{water}}$  values reconstructed using both equations yielded similar  
12 values that are statistically invariant (Tütken, 2003:  $-0.9 \pm 0.3\text{‰}$ ; Lécuyer et al., 1996:  $-0.6 \pm$   
13  $\text{ca. } 0.8\text{‰}$ ).

14

15 In order to assess the possibility of diagenetic alteration of the enamel oxygen isotope  
16 composition, the carbonate ( $\delta^{18}\text{O}_{\text{CO}_3}$ ) and the phosphate ( $\delta^{18}\text{O}_{\text{PO}_4}$ ) group of the enamel were  
17 plotted against each other and compared to a compilation of  $\delta^{18}\text{O}_{\text{CO}_3}$  vs.  $\delta^{18}\text{O}_{\text{PO}_4}$  pairs from  
18 extant mammals published by Pellegrini et al. (2011). The  $\delta^{18}\text{O}_{\text{CO}_3}$  values were determined in  
19 the remaining fraction of the pretreated *H. schinzii* enamel powders. About 800  $\mu\text{g}$  of each  
20 enamel powder sample were analyzed with a Thermo Finnigan MAT 253 gas source isotope  
21 ratio mass spectrometer in continuous flow mode equipped with a GasBench II at the  
22 University of Mainz. The  $\delta^{18}\text{O}_{\text{CO}_3}$  values were measured against VPDB and normalized to a  
23 NBS-18 and NBS-19 calibrated Laaser marble ( $-5.21\text{‰}$ ; replicated precision,  $1\sigma$ , better than  
24  $0.1\text{‰}$ ). Afterward, the results were converted to the SMOW scale using the equation of  
25 Coplen et al. (1983):

$$26 \quad \delta^{18}\text{O}_{\text{SMOW}} = 1.03091 \cdot \delta^{18}\text{O}_{\text{PDB}} + 30.91. \quad (3)$$

27

## 1 **2.5 Mathematical re-sampling of intra-annual isotope data**

2 In bivalves, shell growth rate declines during ontogeny resulting in increasingly narrow  
3 annual growth increments with increasing lifespan (Jones and Quitmyer, 1996). Since the  
4 isotope samples were taken at approximately equidistant intervals (100 to 200  $\mu\text{m}$ ), the  
5 number of samples per year decreases through lifetime and the time represented by each  
6 carbonate sample (= time-averaging) increases in ontogenetically older shell portions. To  
7 compensate for that bias and make the isotope samples from different ontogenetic years  
8 comparable to each other, the number of  $\delta^{18}\text{O}_{\text{shell}}$  values per year was mathematically  
9 equalized by a re-sampling technique similar to that described in Schöne et al. (2004) and  
10 Hallmann et al. (2011). Following previous work (e.g. Schöne and Fiebig, 2008; Wanamaker  
11 et al., 2011), we fitted the isotope data of each annual increment with a 7-point cubic spline  
12 using the software Analyseries 1.1 (Paillard et al., 1996) and re-sampled each intra-annual  
13 curve so that the same number of isotope values were available for each annual increment,  
14 i.e., seven  $\delta^{18}\text{O}_{\text{shell}}$  values. This re-sampling method slightly deviated from previous  
15 approaches (Schöne et al., 2004; Hallmann et al., 2011), because it was impossible to  
16 determine seasonal growth curves from microgrowth patterns. Hence, the  $\delta^{18}\text{O}_{\text{shell}}$  values  
17 within a given year most likely represented different amounts of time, but the first, second,  
18 third etc.  $\delta^{18}\text{O}_{\text{shell}}$  values of different years represented same amounts of time.

19

## 20 **3 Results**

### 21 **3.1 Preservation of material**

22 According to a set of different diagenesis screening tests outlined above, the studied shells of  
23 *Glycymeris planicostalis* from the Rupelian of the Mainz Basin consist of aragonite and were  
24 remarkably well preserved. This even applies to the chalky rims of the shells, i.e., the shell  
25 portions that were only pale blue stained by Mutvei's solution and lost almost all organics  
26 during taphonomy. Orange cathodoluminescence was only emitted from very few isolated  
27 spots, i.e., cracks containing neomorphic mineral phases. Most other portions of the shells  
28 were dark blue to non-luminescent. Moreover, both reflected light microscope and electron  
29 microscope analyses revealed the same shell microstructures that occur in modern  
30 representatives of this genus, i.e., crossed-lamellar structures (Fig.2D-F). Alternately, the 1<sup>st</sup>  
31 order lamellae appear dark and bright because the higher order-lamellae are arranged in a

1 fence-like manner and stand perpendicular to each other (compare Füllenbach et al., 2014).  
2 Furthermore, both shell layers are perforated by numerous hollow microtubuli (Fig. 2G),  
3 especially in the juvenile portion of the shells. On rare occasions, these tubuli (ca. 10µm in  
4 diameter) are filled with pyrite crystals or iron oxides.

5 Like the bivalves, the studied sirenian teeth are well preserved (Fig. 3). The  $\delta^{18}\text{O}_{\text{CO}_3}$  vs.  
6  $\delta^{18}\text{O}_{\text{PO}_4}$  pairs of the seven specimens plot well within the 95% prediction intervals of modern  
7 and other well-preserved fossil mammal enamel data compiled by Pellegrini et al. (2011)  
8 (Table 1; Fig. 3). Diagenetic alteration of tooth enamel would in the first place have affected  
9 the carbonate-bound oxygen (Iacumin et al., 1996) and resulted in  $\delta^{18}\text{O}_{\text{CO}_3}$  vs.  $\delta^{18}\text{O}_{\text{PO}_4}$  pairs  
10 plotting farther away from the regression line depicted in Pellegrini et al. (2011). Given the  
11 excellent preservation,  $\delta^{18}\text{O}_{\text{water}}$  values were computed from  $\delta^{18}\text{O}_{\text{PO}_4}$  values of the enamel  
12 using equation 2. On average, the  $\delta^{18}\text{O}_{\text{water}}$  value of the ambient seawater was  $-0.9 \pm 0.3\text{‰}$   
13 ( $1\sigma$ ).

14

### 15 **3.2 Bivalve sclerochronology: $\delta^{18}\text{O}_{\text{shell}}$ and reconstructed water temperatures**

16 The studied fossil *G. planicostalis* specimens show distinct growth lines in the ventral margin  
17 and the hinge plate of Mutvei-stained cross-sections (Fig. 2H). These lines were previously  
18 identified as periodic annual features (Berthou et al., 1986; Royer et al., 2013; Bušelić et al.,  
19 2014) separating the growth pattern in annual time slices, i.e., annual growth increments. The  
20 annual growth lines are more distinctly developed and hence easier to discern in the hinge  
21 plate than in the ventral margin. Based on annual increment counts, it was possible to  
22 determine the ontogenetic ages of the specimens. Specimens MB-Wht-2, MB-Wht-4 and MB-  
23 Wht-7 reached life spans of 77, 84 and 67 years, respectively.

24 Oxygen isotope curves of all three specimens exhibit distinct seasonal oscillations (16, 14 and  
25 10 cycles in specimens MB-Wht-2, -4, and -7, respectively) with the annual growth lines  
26 occurring shortly after the most negative  $\delta^{18}\text{O}_{\text{shell}}$  values of each cycle (Fig. 4; see  
27 Supplements). In other words, the full seasonal amplitudes are preserved in the shells  
28 including winter and summer values. The annual growth line formation occurred in late  
29 summer/early fall.

1 The shells grew faster during the first half of the year than after summer. This is well reflected  
2 in the seasonal temperature curve based on the averaged  $\delta^{18}\text{O}_{\text{shell}}$  values of all 40 measured  
3 annual increments (Fig. 5). There are more data points in shell portions formed during spring  
4 than in shell portions formed during fall (Fig. 5). Accordingly, the reconstructed temperature  
5 curve is right-skewed.

6 The average annual  $\delta^{18}\text{O}_{\text{shell}}$  values and seasonal  $\delta^{18}\text{O}_{\text{shell}}$  ranges are fairly similar among the  
7 three studied specimens (Table 2). Seasonal extremes fluctuate between -1.48‰ (summer  
8 value) and 0.75‰ (winter value) in specimen MB-Wht-2, between -1.16‰ and 0.67‰ in  
9 specimen MB-Wht-4, and between -1.19‰ and 0.60‰ in specimen MB-Wht-7. Using the  
10 reconstructed  $\delta^{18}\text{O}_{\text{water}}$  value, this translates into total temperature ( $T_{\delta^{18}\text{O}}$ ) ranges of 9.7°C,  
11 7.6°C and 7.8°C in specimens MB-Wht-2, MB-Wht-4 and MB-Wht-7, respectively. Taking  
12 the resampled values of the 40 seasonal cycles of all three specimens, the average annual  
13 temperature is  $15.4 \pm 0.7^\circ\text{C}$  ( $1\sigma$ ), and the seasonal temperature range equals 3.7°C with  
14 average minimum (winter) values of  $13.6 \pm 0.8^\circ\text{C}$  ( $1\sigma$ ) and average maximum (summer)  
15 values of  $17.3 \pm 1.2^\circ\text{C}$  ( $1\sigma$ ). Noteworthy, the seasonal amplitudes vary through time. In some  
16 years, the seasonal  $T_{\delta^{18}\text{O}}$  range was less than 2°C (Fig. 4).

17

## 18 **4 Discussion**

19 As demonstrated by this study, shells of *Glycymeris planicostalis* provide an excellent archive  
20 to reconstruct climate dynamics – in particular changes of sea surface temperature – during  
21 the Oligocene on subseasonal to inter-annual time-scales. Shells of the studied species grew  
22 during both the coldest and warmest periods of the year and therefore contain information on  
23 the full seasonal temperature amplitude over a coherent time interval of several years that  
24 prevailed in the Mainz Basin ~30 Ma ago. Furthermore, the shells are pristinely preserved and  
25 their  $\delta^{18}\text{O}_{\text{shell}}$  values can potentially reflect changes of ambient water temperature.

26

### 27 **4.1 Preservation**

28 According to diagenetic screening the studied *G. planicostalis* shells are well preserved. The  
29 shells consist of pristine aragonite. Furthermore, SEM analysis revealed original delicate shell

1 microstructures including the typical skeletal feature of glycymerids, i.e., microtubuli. These  
2 cylindrical cavities perforate the inner and outer shell layers and are filled with organics  
3 during the lifetime of the animal (e.g., Waller, 1980; Crippa, 2013). The diagenetic loss of  
4 organic material leaves behind hollow cavities that potentially can be filled with neomorphic  
5 mineral phases. However, the microtubuli of the studied specimens were typically hollow and  
6 only rarely contained pyrite. Pyrite crystals can even occur in shells of living bivalves and are  
7 possibly related to the bacterial degradation of organic matter (Clark and Lutz, 1980).

8 In fact, the recovery of pristinely preserved fossil glycymerids has been reported from many  
9 other localities and geological time intervals (e.g., Tsuboi and Hirata, 1935; Crippa, 2013).  
10 Since *Glycymeris* spp. dwell in sandy to fine gravelly habitats, shells of this genus are usually  
11 embedded in coarse grained and highly porous sediments. In such type of host rock and  
12 stratigraphic age, one would not expect aragonitic shell preservation, particularly if the burial  
13 depth is shallow (few tens of meters) and the sediment is still unconsolidated as this is the  
14 case with the weakly cemented sandstones of the Alzey Formation. Under surface conditions,  
15 aragonite is metastable and slowly turns into the more stable polymorph of  $\text{CaCO}_3$ , i.e.,  
16 calcite (Boettcher and Wyllie, 1967). This conversion into calcite can be expedited when a  
17 fluid is present (Putnis and Putnis, 2007) and when temperature is increased (Dasgupta,  
18 1963). The resistance of glycymerid shells against diagenetic alteration likely resulted from  
19 low organic content and the dense crossed-lamellar microstructure (Taylor and Layman,  
20 1972).

21

## 22 **4.2 Timing and rate of shell growth**

23 Pristine preservation is a major prerequisite for the reconstruction of environmental variables  
24 from geochemical properties of the shells including ambient water temperature from  $\delta^{18}\text{O}_{\text{shell}}$   
25 values. According to shell oxygen isotope data the studied shells grew during winter and  
26 summer. Similar findings on shell growth during seasonal extremes were recently reported for  
27 modern *Glycymeris bimaculata* from Croatia (Bušelić et al., 2014). The only difference is that  
28 the Oligocene shells formed annual growth lines in late summer/early fall, whereas the period  
29 of extremely slow or no shell growth in specimens from Croatia occurs during spring. On the  
30 contrary, modern *G. glycymeris* from the North Atlantic form annual growth breaks in winter  
31 (Berthou et al., 1986; Royer et al., 2013). These findings suggest that the timing and rate of

1 shell growth can vary greatly among different species of the same genus and most likely even  
2 among specimens of the same species alive at different localities (e.g., Ansell, 1968; Jones &  
3 Quitmyer, 1996).

4 A number of explanations have been proposed to explain the reason for periodic cessation of  
5 shell growth. Temperature stress seems to limit shell growth in many bivalves. Above and  
6 below a taxon-specific water temperature range, biomineralization ceases and results in the  
7 formation of winter or summer growth lines (Jones and Quitmyer, 1996) or even both  
8 (Schöne et al., 2002). For example, *Mercenaria mercenaria* stops shell growth above 31°C  
9 and below 9°C (Ansell 1968). Following this explanation, modern *G. glycymeris* from the  
10 North Atlantic forms winter lines when temperatures fall below the tolerance limit of this  
11 species, as suggested by Royer et al. (2013). In some taxa, annual growth line formation can  
12 also be linked to the reproductive cycle. For example, *Phacosoma japonicum* from Japan not  
13 only forms winter lines, but also slows down shell growth regularly during June and July, i.e.,  
14 during the peak spawning phase (Sato, 1995). Instead of biomineralizing shell, the energy is  
15 then allocated to the formation of eggs and sperms. Spawning breaks may be limited to  
16 species lacking specific tissues for energy (lipids) storage. Modern *G. glycymeris* from the  
17 North Atlantic, for example, belongs to this group of bivalves and reportedly spawns once or  
18 twice per year between spring and fall (Galap et al. 1997). In the Mediterranean Sea, *G.*  
19 *nummaria* spawns in July and August, followed by a sudden decrease of the condition index  
20 in late summer/fall (Crnčević et al., 2013). However, it has remained unresolved whether  
21 modern *Glycymeris* spp. can only form shell during periods of sexual inactivity. Existing  
22 studies on seasonal shell growth of this genus were based on juvenile specimens or juvenile  
23 portions of adult specimens (Peharda et al., 2012; Bušelić et al., 2014; Royer et al., 2013).  
24 Therefore, it is difficult to draw conclusions on how the reproductive cycle affects seasonal  
25 growth in (modern) *Glycymeris* spp. It is not possible to determine whether growth line  
26 formation of *G. planicostalis* was governed by reproduction or other environmental factors.  
27 At least the annual growth lines in the studied specimens from the Oligocene are unrelated to  
28 seasonal temperature extremes because the lines do not fall together with the most negative  
29 and positive oxygen isotope-derived water temperatures (Fig. 4).

30 Shell growth rates of the studied bivalves from the early Oligocene of the Mainz Basin also  
31 varied during the main growing season. For example, shell production was faster during  
32 spring and summer than during fall and winter. This finding has implications for geochemical

1 sampling strategies. In order to obtain reliable information on the actual seasonal temperature  
2 spread, a higher sampling resolution has to be applied in slow-growing shell portions.

3

#### 4 **4.3 Temperatures of the Mainz Basin during the Rupelian**

5 Only few temperature estimates of the Mainz Basin and adjacent regions during the Rupelian  
6 are currently available. For example, sediments of the Alzey Formation contain a diverse  
7 warm-water fauna including marine fish, mammals and crocodiles as well as terrestrial turtles.  
8 Based on this fossil assemblage, subtropical climate conditions – similar to the modern  
9 southeastern Mediterranean – were inferred for the Mainz Basin (Grimm et al., 2003, 2011).  
10 Furthermore, macroflora and palynological data from the Bodenheim Formation yielded  
11 winter and summer air temperatures of 7.1-10.2°C and 25.7-28.1°C, respectively (Pross et al.,  
12 1998; Pross et al., 2000). These estimates compare well with those obtained from fossil floras  
13 of other contemporaneous localities in Central Europe (Mosbrugger et al., 2005; Erdei et al.,  
14 2012).

15 Knowledge on water temperatures of the Mainz Basin comes from oxygen isotope  
16 compositions of biogenic skeletons. Tütken (2003) reported  $\delta^{18}\text{O}_{\text{PO}_4}$  values of shark teeth that  
17 correspond to absolute temperatures between 6.9° and 23.3°C (temperatures recalculated  
18 assuming a  $\delta^{18}\text{O}_{\text{water}}$  value of -0.9‰; Table 3), using the thermometry equation of Longinelli  
19 and Nuti (1973). Grimm (1994) reported oxygen isotope data of planktonic and benthic  
20 foraminifera that can be converted into absolute temperatures using the paleothermometry  
21 equation by Anderson and Arthur (1983) and a  $\delta^{18}\text{O}_{\text{water}}$  value of -0.9‰. Based on this  
22 calculation, sea surface temperatures of the Mainz Basin fluctuated between 11.7° and 21.3°C  
23 (Table 4), whereas bottom water (up to 150 m depth; Grimm et al., 2011) temperatures were  
24 as cold as 5.9° to 14.9°C during the Rupelian. Similar surface water temperatures were  
25 reconstructed from bivalve shells in the present study (12.3°C and 22.0°C), although the  
26 lowest temperatures are ~5°C higher than those obtained from shark teeth (Fig. 6). Leaving  
27 aside the fact that it is rather unlikely that the studied bivalves, sharks and foraminifera lived  
28 during the exact same time interval, a direct comparison of temperature extremes derived  
29 from the different marine archives seems problematic for a variety of reasons:

1 (i) The temporal resolution provided by foraminifera is much higher than that of bivalves.  
2 Foraminiferan tests can grow within a few weeks (Bé et al., 1981). Thus, each specimen  
3 recorded environmental conditions during a very short time interval of the year. On the  
4 opposite, each sample taken from the bivalve shells represents, on average, about two weeks  
5 to one month worth of growth. Foraminifera samples analyzed so far may not necessarily  
6 have grown when the most extreme seasonal temperatures occurred. Accordingly, actual  
7 winter temperatures may have been slightly colder and summers slightly warmer than  
8 suggested by the  $\delta^{18}\text{O}$  values of foraminifera.

9 (ii) Seasonal temperature extremes given by sharks may not represent the actual temperatures  
10 where the bivalves lived. Being highly mobile, nektonic organisms, the sharks may have  
11 foraged temporarily in the shallowest waters near the coast and at other times dived to the  
12 very bottom of the sea. In addition to vertical movements, they may have travelled large  
13 distances such as modern sharks (e.g., Domeier and Nasby-Lucas, 2008). Lowest  
14 temperatures recorded by sharks may thus represent conditions below the thermocline or  
15 settings much further north instead of winter temperatures in the Mainz Basin. In turn, those  
16 teeth that provided temperature estimates of  $22^\circ\text{C}$  may actually have been formed while the  
17 animals lived in warmer waters farther south or near the coast.

18 (iii) Actual sea surface temperatures during both winter and summer may have been  
19 underestimated by the planktonic foraminifera (and sharks while they resided in shallowest,  
20 coastal waters), because the assumed average  $\delta^{18}\text{O}_{\text{water}}$  value did not reflect the actual isotope  
21 signature of the water. Planktonic foraminifera lived in the upper few meters of the water  
22 column in a narrow, shallow epicontinental sea. In such a habitat, seasonally varying riverine  
23 freshwater influx, precipitation and evaporation rates likely resulted in seasonal changes of  
24 the  $\delta^{18}\text{O}_{\text{water}}$  value. Increased evaporation during summer may have shifted the  $\delta^{18}\text{O}_{\text{water}}$  value  
25 toward more positive values resulting in lower than actual reconstructed water temperatures  
26 near sea surface. In contrast, higher precipitation rates during winter may have shifted the  
27  $\delta^{18}\text{O}_{\text{water}}$  value toward more negative values so that the oxygen isotope-derived temperatures  
28 appeared colder than they actually were. Indications for a seasonally varying  $\delta^{18}\text{O}_{\text{water}}$  value  
29 come, to some extent, from sirenian teeth. Like their extant relatives, sea cows lived in the  
30 upper ten meters of the ocean and near the coast (Louise Chilvers et al., 2004). Thus, they  
31 have recorded the isotope signature of the near-coastal surface water in which the planktonic  
32 foraminifera (*Globigerina* sp.) lived. Reconstructed  $\delta^{18}\text{O}_{\text{water}}$  values fluctuated between  $-0.2\text{‰}$



1 and -1.4‰. If the latter value reflected conditions during winter and the former during  
2 summer, actual seasonal temperatures in the upper few meters of the Mainz Basin  
3 reconstructed from foraminifera ranged between ca. 11°C and 27°C.

4 (iv) Bivalve shell-based temperature estimates cannot be compared directly to those of  
5 planktonic foraminifera even if the fluctuating  $\delta^{18}\text{O}_{\text{water}}$  values in the upper few meters of the  
6 ocean were precisely known. At ca. 30-40 m water depth, bivalves likely experienced a  
7 smaller seasonal temperature range than organisms in the upper few meters of the sea.

8 The benthic faunal associations of the Mainz Basin have been interpreted as reflecting  
9 paleoclimate conditions similar to those of the modern southeastern Mediterranean Sea  
10 (Grimm et al., 2003, 2011). However, temperature estimates derived from *G. planicostalis*  
11 shells suggest lower water temperatures. According to hydrographical studies from coastal  
12 regions in the northwestern Mediterranean (France) and southeastern Mediterranean  
13 (Lebanon), the temperature in 30 to 40 m water depth is still influenced by surface conditions  
14 (Abboud-Abi Saab et al., 2004). At 35 m water depth, the temperatures off Lebanon ranged  
15 between 16.9° and 29.1°C with an annual average of  $22.5^\circ \pm 4.1^\circ\text{C}$  ( $1\sigma$ ), whereas the coastal  
16 waters off France ranged between 12.3° and 21.8°C with an annual average of  $15.2^\circ \pm 2.2^\circ\text{C}$   
17 ( $1\sigma$ ). Temperatures recorded by *G. planicostalis* lay well within these ranges which would  
18 suggest that water temperatures were more similar to regions in the northwestern  
19 Mediterranean than those from subtropical areas. However, the mean annual precipitation in  
20 the area of Marseille (Mediterranean coast of southern France) equals  $751 \pm 172$  mm (Harris  
21 et al., 2014), which is considerably lower than 1000-1250 mm/a reconstructed precipitation  
22 rates for the hinterland of the Mainz Basin (Pross et al., 1998, 2000). A possible explanation  
23 for the high precipitation rates in Central Europe during the Oligocene has been provided by  
24 Pross and Schmiedl (2002). The deposition of the Alzey Formation and its basinal  
25 counterparts, the Bodenheim Formation, took place during sea-level highstands, which could  
26 have increased the moisture concentration in the atmosphere, and so, intensified rainfalls.  
27 Such linkage between sea level rise and precipitation has recently been postulated for the  
28 early Holocene intensification of the Australian-Indonesian monsoon rainfall (Griffiths et al.,  
29 2009).

30

#### 1   **4.4 Advantages of using shells of *Glycymeris planicostalis* for reconstruction** 2   **of Oligocene climate conditions**

3   The studied specimens of *G. planicostalis* offer a number of advantages over existing marine  
4   paleoclimate archives. As sessile organisms, bivalves record the water properties at a specific  
5   locality and depth throughout their lifetimes. Since their shells grew almost year-round, each  
6   isotope sample can be assigned to a particular season. If preservation permits, daily  
7   microgrowth increments can be employed to temporally contextualize the seasonal shell  
8   growth to the nearest week or so (e.g. Schöne et al., 2005b). Such an internal calendar is  
9   missing in foraminifera.

10   The studied *G. planicostalis* specimens lived for several decades and recorded seasonal  
11   temperature changes over the course of many consecutive years. This is a clear advantage  
12   over other climate archives that only provide very short temporal snapshots of unknown  
13   timing within the year such as foraminifera or shark teeth, or few consecutive years, such as  
14   fish otoliths. Analogously to bivalve shells, they form growth lines, and their oxygen isotope  
15   composition can be used for seasonal paleotemperature reconstructions, for example, at the  
16   Eocene/Oligocene boundary (Ivany et al., 2000). Although fish otoliths are very common  
17   components of marine nektonic microfossil assemblages, their reduced size makes them  
18   difficult to sample, and analyses of their chemical composition usually cover only short time  
19   intervals.

20   Long proxy records offer the possibility to track variability of winter and summer  
21   temperatures over the course of several years. Future studies should generate  $\delta^{18}\text{O}_{\text{shell}}$  time-  
22   series of *G. planicostalis* that are long enough to permit spectral analyses. These data should  
23   then be combined with numerical climate models for that time. Furthermore,  $\delta^{18}\text{O}_{\text{shell}}$   
24   chronologies should also be compared to increment widths in order to identify potential  
25   influences of temperature on shell growth rates.

26   The  $\delta^{18}\text{O}_{\text{water}}$  value at 30-40 m water depth was most probably much less variable than near  
27   the sea surface. Seasonal changes in freshwater influx into the Mainz Basin likely did not  
28   have any significant effect on the isotope signature of the water in which the bivalves lived. In  
29   fact, modern *G. glycymeris* from the North Atlantic is most prolific in water with stable  
30   salinity of 34-35 (Rombouts et al., 2012). If the same preference is true for the Oligocene  
31   relatives of this genus, water temperatures can be reconstructed with smaller error bars from

1 oxygen isotope values of the bivalve shells than from skeletal hard parts of nektonic and  
2 planktonic organisms. Evidently, absolute temperature estimates from  $\delta^{18}\text{O}$  values require  
3 knowledge of the oxygen isotope composition of the ambient water, which is rarely available  
4 for fossil environments. In the present study, the  $\delta^{18}\text{O}_{\text{water}}$  value was reconstructed from the  
5 tooth enamel of sea cows from the same stratigraphic level. Although the bivalves and the sea  
6 cows did most certainly not live during the exact same time and the sphere of action of the sea  
7 cows was the upper ten meters of the ocean, the average  $\delta^{18}\text{O}_{\text{PO}_4}$  value of the sirenian teeth  
8 serves as a reasonable estimate of the Rupelian  $\delta^{18}\text{O}_{\text{water}}$  value (-0.9‰) of the Mainz Basin. A  
9 similar value (-1‰) was also assumed by Grimm (1994). For comparison, the  $\delta^{18}\text{O}_{\text{water}}$  of the  
10 open ocean was -0.5‰ at that time (Lear et al., 2000). To test the temperature estimates  
11 obtained from  $\delta^{18}\text{O}_{\text{shell}}$  values and circumvent uncertainties related to the precise  $\delta^{18}\text{O}_{\text{water}}$   
12 signature during shell formation, future studies should explore other potential temperature  
13 proxies such as Sr/Ca and  $\Delta_{47}$  values (Eagle et al., 2013).

14

## 15 **5 Summary and conclusions**

16 Shells of *Glycymeris planicostalis* serve as excellent recorders of sea surface temperatures in  
17 the Mainz Basin during the Rupelian stage. Since the shells were preserved as pristine  
18 aragonite, the  $\delta^{18}\text{O}_{\text{shell}}$  values can be used to reconstruct ambient water temperature. The  
19  $\delta^{18}\text{O}_{\text{water}}$  value for the temperature calculation was reconstructed using tooth enamel  $\delta^{18}\text{O}_{\text{PO}_4}$   
20 values of the sea cow *Halitherium schinzii* from the same strata. Although the exact oxygen  
21 isotope signature of the water is not known, it is highly likely to assume that the  $\delta^{18}\text{O}_{\text{water}}$   
22 value in 30-40 m water depth, in which *G. planicostalis* lived, remained largely invariant  
23 through time. Attributed to its notable longevity, shells of this species can be used to study  
24 seasonal temperature changes over several consecutive years, even up to decades. As shown  
25 in the present study, summer and winter temperatures varied greatly from year to year. As yet,  
26 such data are hardly available from any other paleoclimate archive of the Oligocene. Such  
27 information can be highly relevant for numerical climate studies aiming to predict possible  
28 future climates in a unipolar glaciated or polar ice-free world.

29

## 30 **Acknowledgements**

1 Two anonymous reviewers and Donna Surge kindly provided comments that helped to further  
2 improve the manuscript. We gratefully acknowledge the assistance of Christoph Füllenbach,  
3 Hilmar A. Holland and Soraya Marali during shell preparation and SEM work. We also thank  
4 Thomas Schindler for his comments and for providing some of the sirenian teeth.  
5 Furthermore, we thank Michael Maus for his help with isotope analyses. This study has been  
6 made possible by a German Research Foundation (DFG) grant to BRS (SCHO 793/11-1) and  
7 JP (PR 651/14-1).

8

## 9 **References**

- 10 Abboud-Abi Saab, M., Romano, J.-C., Bensoussan, N. and Fakhri, M.: Suivis temporels comparés de  
11 la structure thermique d'eaux côtières libanaises (Batroun) et françaises (Marseille) entre juin 1999 et  
12 octobre 2002, C. R. Geosci., 336, 1379–1390, 2004. (in French).
- 13 Anderson, T. F. and Arthur, M. A.: Stable isotopes of oxygen and carbon and their application to  
14 sedimentologic and paleoenvironmental problems, SEPM Short Course, 10, 1–151, 1983.
- 15 Ansell, A. D.: The rate of growth of the hard clam *Mercenaria mercenaria* (L) throughout the  
16 geographical range. J. Cons. Perm. Int. Explor. Mer, 31, 364–409, 1968.
- 17 Ansell, A. D. and Trueman, E. R.: Observations on burrowing in *Glycymeris glycymeris* (L.)  
18 (Bivalvia, Arcacea), J. Exp. Mar. Bio. Ecol., 1, 65–75, 1967.
- 19 Barbosa, S. M.: Decadal variability in Europe's seasons, EGU General Assembly Conference, 19-24  
20 April 2009, Vienna, Austria EGU2009-5332-2, 2009.
- 21 Bé, A. W. H., Caron, D. A. and Anderson, O. R.: Effects of feeding frequency on life processes of the  
22 planktonic foraminifer *Globigerinoides sacculifer* in laboratory culture, J. Mar. Biol. Assoc. UK., 61,  
23 257–277, 1981.
- 24 Berger, J.-P., Reichenbacher, B., Becker, D., Grimm, M. C., Grimm, K. I., Picot, L., Storni, A.,  
25 Pirkenseer, C., Derer, C. and Schaefer, A.: Paleogeography of the Upper Rhine Graben (URG) and the  
26 Swiss Molasse Basin (SMB) from Eocene to Pliocene, Int. J. Earth Sci., 94, 697–710, 2005a.
- 27 Berger, J.-P., Reichenbacher, B., Becker, D., Grimm, M. C., Grimm, K. I., Picot, L., Storni, A.,  
28 Pirkenseer, C. and Schaefer, A.: Eocene-Pliocene time scale and stratigraphy of the Upper Rhine  
29 Graben (URG) and the Swiss Molasse Basin (SMB), Int. J. Earth Sci., 94, 711–731, 2005b.
- 30 Berthou, P., Blanchard, M., Noel, P. and Vergnaud-Grazzini, C.: The analysis of stable isotopes of the  
31 shell applied to the determination of the age of four bivalves of the “Normano-Breton” gulf, Western  
32 Channel, International Council for the Exploration of the Sea, Shellfish Committee, Copenhagen,  
33 Denmark, Annual Report, 1986/K:16, 1–13, 1986.

- 1 Beyrich, E.: Über die Stellung der hessischen Tertiärbildungen, Bericht über die zur Bekanntmachung  
2 geeigneten Verhandlungen der Königlich Preußischen Akademie der Wissenschaften zu Berlin,  
3 Germany, 640–666, 1854. (in German).
- 4 Black, B. A., Gillespie, D. C., MacLellan, S. E. and Hand, C. M.: Establishing highly accurate  
5 production-age data using the tree-ring technique of crossdating: a case study for Pacific geoduck  
6 (*Panopea abrupta*), *Can. J. Fish. Aquat. Sci.*, 65, 2572–2578, 2008.
- 7 Boettcher, A. L. and Wyllie, P. J.: Revision of the calcite-aragonite transition, with the location of a  
8 triple point between calcite I, calcite II and aragonite, *Nature*, 213, 792–793, 1967.
- 9 Brocas, W. M., Reynolds, D. J., Butler, P. G., Richardson, C. A., Scourse, J. D., Ridgway, I. D. and  
10 Ramsay, K.: The dog cockle, *Glycymeris glycymeris* (L.), a new annually-resolved sclerochronological  
11 archive for the Irish Sea, *Palaeogeogr. Palaeoclimatol. 373*, 133–140, 2013.
- 12 Bušelić, I., Peharda, M., Reynolds, D. J., Butler, P. G., González, A. R., Ezgeta-Balić, D., Vilibić, I.,  
13 Grbec, B., Hollyman, P. and Richardson, C. A.: *Glycymeris bimaculata* (Poli, 1795) - A new  
14 sclerochronological archive for the Mediterranean?, *J. Sea Res.*, 95, 139–148, 2015.
- 15 Butler, P. G., Wanamaker, A. D., Scourse, J. D., Richardson, C. A. and Reynolds, D. J.: Variability of  
16 marine climate on the North Icelandic Shelf in a 1357-year proxy archive based on growth increments  
17 in the bivalve *Arctica islandica*, *Palaeogeogr. Palaeoclimatol. 373*, 141–151, 2013.
- 18 Cai, W. and Chu, P. C.: Oceanic responses to gradual transitions of equator-to-pole, *Q. J. Roy. Meteor.*  
19 *Soc.*, 124, 2817–2828, 1998.
- 20 Casey, R.: The stratigraphical palaeontology of the Lower Greensand, *Palaeontology*, 3, 487–621,  
21 1961.
- 22 Chenery, C., Müldner, G., Evans, J., Eckardt, H. and Lewis, M.: Strontium and stable isotope  
23 evidence for diet and mobility in Roman Gloucester, UK, *J. Archaeol. Sci.*, 37, 150–163, 2010.
- 24 Clark, G. R. and Lutz, R. A.: Pyritization in the shells of living bivalves, *Geology*, 8, 268–271, 1980.
- 25 Clementz, M. T. and Koch, P. L.: Differentiating aquatic mammal habitat and foraging ecology with  
26 stable isotopes in tooth enamel, *Oecologia*, 129, 461–472, 2001.
- 27 Clementz, M. T. and Sewall, J. O.: Latitudinal gradients in greenhouse seawater  $\delta^{18}\text{O}$ : evidence from  
28 Eocene sirenian tooth enamel, *Science*, 332, 455–458, 2009.
- 29 Clementz, M. T., Goswami, A., Gingerich, P. D. and Koch, P. L.: Isotopic records from early whales  
30 and sea cows : contrasting patterns of ecological transition, *J. Vertebr. Paleontol.*, 26, 355–370, 2006.
- 31 Coplen, T. B., Kendall, C. and Hopple, J.: Comparison of stable isotope reference samples, *Nature*,  
32 302, 236–238, 1983.
- 33 Crippa, G.: The shell ultrastructure of the genus *Glycymeris* DA COSTA, 1778: a comparison between  
34 fossil and recent specimens, *Riv. Ital. Paleontol. e S.*, 119, 387–399, 2013.
- 35 Crnčević, M., Peharda, M., Ezgeta-Balić, D., and Pećarević, M.: Reproductive cycle of *Glycymeris*  
36 *nummaria* (Mollusca: Bivalvia) from Mali Ston Bay, Adriatic Sea, Croatia, *Sci. Mar.*, 77, 293–300,  
37 2012.

- 1 Dai, A., Fung, I. Y. and Del Genio, A. D.: Surface observed global land precipitation variations during  
2 1900-88, *J. Climate*, 10, 2943–2962, 1997.
- 3 Dasgupta, D. R.: The oriented transformation of aragonite into calcite, *Miner. Mag.*, 33, 924–928,  
4 1963.
- 5 Dettman, D. L., Reische, A. K. and Lohmann, K. C.: Controls on the stable isotope composition of  
6 seasonal growth bands in aragonitic fresh-water bivalves (unionidae), *Geochim. Cosmochim. Ac.*, 63,  
7 1049–1057, 1999.
- 8 Dettman, D. L., Kohn, M. J., Quade, J., Ryerson, F. J., Ojha, T. P. and Hamidullah, S.: Seasonal stable  
9 isotope evidence for a strong Asian monsoon throughout the past 10.7 m.y., *Geology*, 29, 31–34,  
10 2001.
- 11 Dèzes, P., Schmid, S. M. and Ziegler, P. A.: Evolution of the European Cenozoic Rift System:  
12 interaction of the Alpine and Pyrenean orogens with their foreland lithosphere, *Tectonophysics*, 389,  
13 1–33, 2004.
- 14 Domeier, M. and Nasby-Lucas, N.: Migration patterns of white sharks *Carcharodon carcharias*  
15 tagged at Guadalupe Island, Mexico, and identification of an eastern Pacific shared offshore foraging  
16 area, *Mar. Ecol. Prog. Ser.*, 370, 221–237, 2008.
- 17 Eagle, R. A., Eiler, J. M., Tripathi, A. K., Ries, J. B., Freitas, P. S., Hiebenthal, C., Wanamaker Jr., A.  
18 D., Taviani, M., Elliot, M., Marensi S., Nakamura, K., Ramirez, P. and Roy K.: The influence of  
19 temperature and seawater carbonate saturation state on <sup>13</sup>C-<sup>18</sup>O bond ordering in bivalve mollusks,  
20 *Biogeosciences*, 10, 4591-4606, 2013.
- 21 Epstein, S., Buchsbaum, R., Lowenstam, H. and Urey, H.: Revisited carbonate-water isotopic  
22 temperature scale, *B. Am. Meteorol. Soc.*, 64, 1315–1326, 1953.
- 23 Erdei, B., Utescher, T., Hably, L., Tamás, J., Roth-Nebelsick, A. and Grein, M.: Early Oligocene  
24 continental climate of the Palaeogene Basin (Hungary and Slovenia) and the surrounding area, *Turk. J.*  
25 *Earth Sci.*, 21, 153–186, 2012.
- 26 Feigl, F. (Eds.): *Spot tests in inorganic analysis*. Fifth enlarged and revisited english edition, Elsevier  
27 Pub. Co., Amsterdam, Netherland, 1958.
- 28 Flügel, E. (Eds.): *Microfacies of carbonate rocks: analysis, interpretation and application*, Springer,  
29 Berlin, Germany, 2004.
- 30 Füllenbach, C. S., Schöne, B. R. and Branscheid, R.: Microstructures in shells of the freshwater  
31 gastropod *Viviparus viviparus*: A potential sensor for temperature change?, *Acta Biomater.*, 1, 3911–  
32 3921, 2014.
- 33 Galap, C., Leboulenger, F. and Grillot, J.-P.: Seasonal variations in biochemical constituents during  
34 the reproductive cycle of the female dog cockle *Glycymeris glycymeris*, *Mar. Biol.*, 129, 625–634,  
35 1997.
- 36 Gillet, S.: Études sur les Lamellibranches néocomiens, *Mem. S. Geo. F.*, 1, 1–324, 1924. (in French).
- 37 Gradstein, F. M., Ogg, J. G. and Smith, A. G.: *A geologic time scale 2004*, Cambridge University  
38 Press, Cambridge, United Kingdom and New York, NY, USA., 2004.

- 1 Griffiths, M. L., Drysdale, R. N., Gagan, M. K., Zhao, J.-X., Ayliffe, L. K., Hellstrom, J. C., Hantoro,  
2 W. S., Frisia, S., Feng, Y. -x., Cartwright, I., Pierre, E. St., Fischer, M. J. and Suwargadi, B. W.:  
3 Increasing Australian-Indonesian monsoon rainfall linked to early Holocene sea-level rise, *Nat.*  
4 *Geosci.*, 2, 636–639, 2009.
- 5 Grimm, K. I.: Paläoökologie, Paläogeographie und Stratigraphie im Mainzer Becken, im  
6 Oberrheingraben, in der Hessischen Senke und in der Leipziger Bucht während des Mittleren  
7 Rupeltons (Fischschiefer/Rupelium/Unteroligozän), *Mitteilungen Pollichia*, 81, 7–193, 1994. (in  
8 German).
- 9 Grimm, K. I.: Correlation of Rupelian coastal and basin facies in the Mainz Basin (Oligocene,  
10 Germany), *N. Jb. Geol. Paläont. Mitt.*, 3, 146–156, 1998.
- 11 Grimm, K. I.: Foraminiferal zonation of early Oligocene deposits (Selztal Group, Latdorfian,  
12 Rupelian) in the Mainz Basin, Germany, *J. Micropalaeontol.*, 21, 67–74, 2002.
- 13 Grimm, K. I.: Meeresverbindungen im Rupelium Mitteleuropas - Paläobiogeographische  
14 Untersuchungen anhand von Foraminiferen, *Geologisches Jahrbuch Hessen*, 133, 19–27, 2006. (in  
15 German).
- 16 Grimm, K. I., Grimm, M. C. and Schindler, T.: Lithostratigraphische Gliederung im  
17 Rupelium/Chattium des Mainzer Beckens, Deutschland., *N. Jb. Geol. Paläont. Abh.*, 218, 343–397,  
18 2000. (in German).
- 19 Grimm, K. I., Grimm, M. C., Neuffer, F. O. and Luty, H.: Die fossilen Wirbelloses Mainzer  
20 Tertiärbeckens Teil 1-1 Geologischer Führer durch das Mainzer Tertiärbecken, *Mainzer*  
21 *Naturwissenschaftliches Archiv - Beiheft*, 26, 1–158, 2003. (in German)
- 22 Grimm, K. I., Grimm, M., Radtke, G., Kadolsky, D., Schäfer, P., Franzen, J. L., Schindler, T. and  
23 Hottenrott Martin: Mainzer Becken, in: *Stratigraphie von Deutschland IX. Tertiär, Teil 1*, Deutsche  
24 *Stratigraphische Kommission (Eds.) - Schriftenreihe der Deutschen Gesellschaft für*  
25 *Geowissenschaften*, 75, 133–209, 2011. (in German).
- 26 Grossman, E. L. and Ku, T.-L.: Oxygen and carbon isotope fractionation in biogenic aragonite:  
27 temperature effects, *Chem. Geol.*, 59, 59–74, 1986.
- 28 Grossman, E. L., Mii, H.-Zhang, C. and Yancey, T. E.: Chemical variation in Pennsylvanian  
29 brachiopod shells – diagenetic, taxonomic, microstructural, and seasonal effects, *J. Sed.*, 66, 1011–  
30 1022, 1996.
- 31 Hallmann, N., Schöne, B. R., Irvine, G. V., Burchell, M., Cokelet, E. D. and Hilton, M. R.: An  
32 improved understanding of the Alaska Coastal Current: The application of a bivalve growth-  
33 temperature model to reconstruct freshwater-influenced paleoenvironments, *Palaios*, 26, 346–363,  
34 2011.
- 35 Hansen, B., Østerhus, S., Quadfasel, D. and Turrel, W.: Already the Day After Tomorrow?, *Science*,  
36 305, 953–954, 2004.
- 37 Haq, B. U., Hardenbol, J. and Vail, P. R.: Mesozoic and Cenozoic chronostratigraphy and cycles of  
38 Sea-Level change, in: *Sea-level changes: an integrated approach*, Wilgus, C. K., Hasting, B. S.,  
39 Posamentier, H., Van Wagoner, J., Ross, C. K. and Kendall, C. G. S. C, *SEPM Spec. Publ.*, 42, 71–  
40 108, 1988.

- 1 Harris, I., Jones, P. D., Osborn, T. J. and Lister, D. H.: Updated high-resolution grids of monthly  
2 climatic observations - the CRU TS3.10 Dataset, *Int. J. Climatol.*, 34, 623–642, 2014.
- 3 Hátún, H., Sandø, A. B., Drange, H., Hansen, B. and Valdimarsson, H.: Influence of the Atlantic  
4 subpolar gyre on the thermohaline circulation, *Science*, 309, 1841–1844, 2005.
- 5 Hurrell, J. W.: Decadal trends in the North Atlantic Oscillation: regional temperatures and  
6 precipitation, *Science*, 269, 676–679, 1995.
- 7 Iacumin, P., Bocherens, H., Mariotti, A. and Longinelli, A.: Oxygen isotope analyses of co-existing  
8 carbonate and phosphate in biogenic apatite: a way to monitor diagenetic alteration of bone  
9 phosphate?, *Earth Planet. Sci. Lett.*, 142, 1–6, 1996.
- 10 Ivany, L. C., Patterson, W. P. and Lohmann, K. C.: Cooler winters as a possible cause of mass  
11 extinctions at the Eocene/Oligocene boundary, *Nature*, 407, 887–890, 2000.
- 12 Jones, D. S. and Quitmyer, I. R.: Marking time with bivalve shells: oxygen isotopes and season of  
13 annual increment formation, *Palaios*, 11, 340–346, 1996.
- 14 Lawrimore, J. H. , Menne, M. J., Gleason, B. E., Williams, C. N., Wuertz, D. B., Vose, R. S., and  
15 Rennie, J.: An overview of the Global Historical Climatology Network 25 monthly mean temperature  
16 data set, version 3, *J. Geophys. Res.*, 116, D19121, doi:10.1029/2011JD016187, 2011.
- 17 Lear, C. H., Elderfield, H. and Wilson, P. A.: Cenozoic deep-sea temperatures and global ice volumes  
18 from Mg/Ca in benthic foraminiferal Calcite, *Science*, 287, 269-272, 2000.
- 19 Lécuyer, C., Grandjean, P., O’Neil, J. R., Cappetta, H. and Martineau, F.: Thermal excursions in the  
20 ocean at the Cretaceous - Tertiary boundary (northern Morocco):  $\delta^{18}\text{O}$  record of phosphatic fish  
21 debris, *Palaeogeogr. Palaeoclimatol.*, 105, 235–243, 1993.
- 22 Lécuyer, C., Grandjean, P., Paris, F., Robardet, M. and Robineau, D.: Deciphering “temperature” and  
23 “salinity” from biogenic phosphates: the  $\delta^{18}\text{O}$  of coexisting fishes and mammals of the Middle  
24 Miocene sea of western France, *Palaeogeogr. Palaeoclimatol.*, 126, 61–74, 1996.
- 25 Lefebvre, V., Donnadieu, Y., Goddérès, Y., Fluteau, F. and Hubert-Théou, L.: Was the Antarctic  
26 glaciation delayed by a high degassing rate during the early Cenozoic?, *Earth Planet. Sci. Lett.*, 371-  
27 372, 203–211, 2013.
- 28 Longinelli, A. and Nuti, S.: Revisited phosphate-water isotopic temperature scale, *Earth Planet. Sci.*  
29 *Lett.*, 19, 373–376, 1973.
- 30 Louise Chilvers, B., Delean, S., Gales, N. J., Holley, D. K., Lawler, I. R., Marsh, H. and Preen, A. R.:  
31 Diving behaviour of dugongs, *Dugong dugon*, *J. Exp. Mar. Biol. Ecol.*, 304, 203–224, 2004.
- 32 Machel, H. G., Mason, R. A., Mariano, A. N. and Mucci, A.: Causes and emission of luminescence in  
33 calcite and dolomite, in: *Luminescence microscopy and spectroscopy: qualitative and quantitative*  
34 *applications*, Barker, C. E., and Kopp, O. C., SEPM Short, Tulsa, Oklahoma, USA, 25, 9–173, 1991.
- 35 Major, R. P.: Cathodoluminescence in post-Miocene carbonates, in: *Luminescence microscopy and*  
36 *spectroscopy: qualitative and quantitative applications*, Barker, C. E. and Kopp, O. C., SEPM Short,  
37 Tulsa, Oklahoma, USA, 25, 149–155, 1991.



- 1 Marshall, J., Kushnir, Y., Battisti, D., Chang, P., Czaja, A., Dickson, R., Hurrell, J. W., McCartney,  
2 M., Saravanan, R. and Visbeck, M.: North Atlantic climate variability: phenomena, impacts and  
3 mechanisms, *Int. J. Climatol.*, 21, 1863–1898, 2001.
- 4 Martini, E.: Bestandsaufnahme des Nannoplankton im “prä-aquitane” Tertiär des Mainzer Beckens,  
5 *Mainzer geowissenschaftliche Mitteilungen*, 10, 29–36, 1982. (in German).
- 6 Martini, E. and Müller, C.: Das marine Alttertiär in Deutschland und seine Einordnung in die Standard  
7 Nannoplankton Zonen, *Erdol und Kohle*, 24, 381–384, 1971. (in German).
- 8 Miller, K. G., Kominz, M. A., Browning, J. V., Wright, J. D., Mountain, G. S., Katz, M. E., Sugarman,  
9 P. J., Cramer, B. S., Christie-Blick, N. and Pekar, S. F.: The Phanerozoic record of global sea-level  
10 change, *Science*, 310, 1293–1298, 2005.
- 11 Mosbrugger, V., Utescher, T. and Dilcher, D. L.: Cenozoic continental climatic evolution of Central  
12 Europe, *Proc. Natl. Acad. Sci. USA*, 102, 14964–14969, 2005.
- 13 O’Neil, J. R., Roe, L. J., Reinhard, E. and Blakes, R. E.: A rapid and precise method of oxygen isotope  
14 analysis of biogenic phosphate, *Israel J. Earth Sci.*, 43, 203–212, 1994.
- 15 Ottersen, G., Planque, B., Belgrano, A., Post, E., Reid, P. and Stenseth, N.: Ecological effects of the  
16 North Atlantic Oscillation, *Oecologia*, 128, 1–14, 2001.
- 17 Paillard, D., Labeyrie, L. and Yiou, P.: Macintosh program performs time-series analysis, *Eos*  
18 *Transaction of the American Geophysical Union*, 77, 379, 1996.
- 19 Pälike, H., Norris, R. D., Herrle, J. O., Wilson, P. A., Coxall, H. K., Lear, C. H., Shackleton, N. J.,  
20 Tripathi, A. K. and Wade, B. S.: The heartbeat of the Oligocene climate system, *Science*, 314, 1894–  
21 1898, 2006.
- 22 Peharda, M., Crnčević, M., Bušelić, I., Richardson, C.A., and Ezgeta-Balic, D.: Growth and longevity  
23 of *Glycymeris nummaria* (Linnaeus, 1758) from the eastern Adriatic, Croatia, *J. Shellfish Res.*, 31,  
24 947–950, 2012.
- 25 Pellegrini, M., Lee-Thorp, J. A. and Donahue, R. E.: Exploring the variation of the  $\delta^{18}\text{O}_p$  and  $\delta^{18}\text{O}_c$   
26 relationship in enamel increments, *Palaeogeogr. Palaeoclimatol.*, 310, 71–83, 2011.
- 27 Picot, L.: Le Paléogène des synclinaux du Jura et de la bordure sud-rhénane: Paléontologie  
28 (Ostracodes), paléoécologie, biostratigraphie, paléogéographie, *GeoFocus*, 5, 1–240, 2002. (in  
29 French).
- 30 Pross, J.: Aquatische Palynomorphen im Rupel des Mainzer Beckens (Oligozän, Südwestdeutschland):  
31 Paläoökologie, Biostratigraphie und Taxonomie., *Tübinger Mikropaläontologische Mitteilungen*, 15,  
32 1–181, 1997. (in German).
- 33 Pross, J.: Paleo-oxygenation in Tertiary epeiric seas: evidence from dinoflagellate cysts, *Palaeogeogr.*  
34 *Palaeoclimatol.*, 166, 369–381, 2001.
- 35 Pross, J. and Schmiedl, G.: Early Oligocene dinoflagellate cysts from the Upper Rhine Graben (SW  
36 Germany): paleoenvironmental and paleoclimatic implications, *Mar. Micropaleontol.*, 45, 1–24, 2002.

- 1 Pross, J., Bruch, A. A., Mosbrugger, V. and Kvacek, Z.: Paleogene pollen and spores as a tool for  
2 quantitative paleoclimate reconstructions: the Rupelian (Oligocene) of Central Europe, in: Goodman,  
3 D. K., and Clarke, R. T., Proceedings of the Ninth International Palynological Congress, Houston,  
4 Texas, USA, 1996, 23-28 June 1996, American Association of Stratigraphic Palynologists Foundation,  
5 299–310, 2000.
- 6 Pross, J., Bruch, A. and Kvaček, Z.: Paläoklima-Rekonstruktionen für den Mittleren Rupelton (Unter-  
7 Oligozän) des Mainzer Beckens auf der Basis mikro-und makrobotanischer Befunde, Mainzer  
8 Geowissenschaftliche Mitteilungen, 27, 79–92, 1998.(in German).
- 9 Putnis, A. and Putnis, C. V.: The mechanism of reequilibration of solids in the presence of a fluid  
10 phase, J. Solid State Chem., 180, 1783–1786, 2007.
- 11 Ramsay, K., Kaiser, M. J., Richardson, C. A., Veale, L. O. and Brand, A. R.: Can shell scars on dog  
12 cockles (*Glycymeris glycymeris* L.) be used as an indicator of fishing disturbance?, J. Sea Res., 43,  
13 167–176, 2000.
- 14 Raper, S. C. B. and Braithwaite, R. J.: Low sea level rise projections from mountain glaciers and  
15 icecaps under global warming, Nature, 439, 311–313, 2006.
- 16 Ritzkowski, S.: Das Tertiär der Hessischen Senke in der Stratigraphischen Tabelle von Deutschland  
17 2002, Newsl. Stratigr., 41, 339–346, 2005.
- 18 Rombouts, I., Beaugrand, G. and Dauvin, J.-C.: Potential changes in benthic macrofaunal distributions  
19 from the English Channel simulated under climate change scenarios, Estuar. Coast. Shelf Sci., 99,  
20 153–161, 2012.
- 21 Ropes, J. W.: Modern methods used to age oceanic bivalves, Nautilus, 99, 53–57, 1985.
- 22 Royer, C., Thébault, J., Chauvaud, L. and Olivier, F.: Structural analysis and paleoenvironmental  
23 potential of dog cockle shells (*Glycymeris glycymeris*) in Brittany, northwest France, Palaeogeogr.  
24 Palaeocl., 373, 123–132, 2013.
- 25 Sato, S.: Spawning periodicity and shell microgrowth patterns of the venerid bivalve *Phacosoma*  
26 *japonicum* (Reeve, 1850), Veliger, 38, 61–72, 1995.
- 27 Schindler, T., Poschmann, M. and Wuttke, M.: Chondrichthyan feeding depressions in a subtidal  
28 coastal environment from the Mainz Basin (Oligocene, SW Germany), N. Jb. Geol. Paläont. Abh.,  
29 237, 29–39, 2005.
- 30 Schöne, B. R., Goodwin, D. H., Flessa, K. W., Dettman, D. L., and Roopnarine, P. D.:  
31 Sclerochronology and growth of the bivalve mollusks *Chione* (*Chionista*) *fluctifraga* and *C.*  
32 (*Chionista*) *cortezii* in the northern Gulf of California, Mexico, Veliger, 45, 45–54, 2002.
- 33 Schöne BR, Freyre Castro AD, Fiebig J, Houk SD, Oschmann W and Kröncke I.: Sea surface water  
34 temperatures over the period 1884-1983 reconstructed from oxygen isotope ratios of a bivalve mollusk  
35 shell (*Arctica islandica*, southern North Sea). Palaeogeogr. Palaeocl., 212, 215–232, 2004.
- 36 Schöne, B. R., Dunca, E., Fiebig, J. and Pfeiffer, M.: Mutvei's solution: An ideal agent for resolving  
37 microgrowth structures of biogenic carbonates, Palaeogeogr. Palaeocl., 228, 149–166, 2005a.

- 1 Schöne, B. R., Houk, S. D., Freyre Castro, A. D., Fiebig, J., Oschmann, W., Kroncke, I., Dreyer, W.  
2 and Gosselck, F.: Daily growth rates in shells of *Arctica islandica*: assessing sub-seasonal  
3 environmental controls on a long-lived bivalve mollusk, *Palaios*, 20, 78–92, 2005b.
- 4 Schöne, B. R. and Fiebig, J.: Seasonality in the North Sea during the Allerød and Late Medieval  
5 Climate Optimum using bivalve sclerochronology, *Int. J. Earth Sci.*, 98, 83–98, 2008.
- 6 Sissingh, W.: Tertiary paleogeographic and tectonostratigraphic evolution of the Rhenish Triple  
7 Junction, *Palaeogeogr. Palaeoclimatol.*, 196, 229–263, 2003.
- 8 Solomon, S., Qin, D., Manning, Z., Chen, M., Marquis, K.B., Averyt, M., Tignor and H.L. Miller  
9 (Eds.): Contribution of Working Group I to the Fourth Assessment Report of the Intergovernmental  
10 Panel on Climate Change, 2007, Cambridge University Press, Cambridge, UK and New York, NY,  
11 USA., 2007.
- 12 Spiegel, C., Kuhlemann, J. and Frisch, W.: Tracing sediment pathways by zircon fission track  
13 analysis: Oligocene marine connections in Central Europe, *Int. J. Earth Sci.*, 96, 363–374, 2007.
- 14 Stenseth, N. C., Mysterud, A., Ottersen, G., Hurrell, J. W., Chan, K.-S. and Lima, M.: Ecological  
15 effects of climate fluctuations, *Science*, 297, 1292–1296, 2002.
- 16 Strom, A., Francis, R. C., Mantua, N. j, Miles, E. L. and Peterson, D. L.: North Pacific climate  
17 recorded in growth rings of geoduck clams: A new tool for paleoenvironmental reconstruction,  
18 *Geophys. Res. Lett.*, 31, L06206, 2004.
- 19 Taylor, J. D. and Layman, M.: The mechanical properties of bivalve (Mollusca) shell structures,  
20 *Palaeontol.*, 15, 73–87, 1972.
- 21 Thewissen, J. G. M., Cooper, L. N., Clementz, M. T., Bajpai, S. and Tiwari, B. N.: Whales originated  
22 from aquatic artiodactyls in the Eocene epoch of India, *Nature*, 450, 1190–1194, 2007.
- 23 Thomas, R. D. K.: Functional morphology, ecology, and evolutionary conservatism in the  
24 *Glycymerididae* (Bivalvia), *Palaeontol.*, 18, 217–254, 1975.
- 25 Thomas, R. D. K.: Shell form and the ecological range of living and extinct *Arcoidea*, *Paleobiol.*, 4,  
26 181–194, 1978.
- 27 Tsuboi, C. and Hirata, M.: Arrangement of micro-crystals of calcium carbonate in some fossil shells,  
28 *Glycymeris yessoensis* SOWERBY, B. *Earthq. Res. I. Tokyo*, 13, 660–664, 1935.
- 29 Tütken, T.: Die Bedeutung der Knochenfrühdiagenese für die Erhaltungsfähigkeit in vivo erworbener  
30 Element- und Isotopenzusammensetzungen in fossilen Knochen, Doctoral Thesis, Eberhard-Karls-  
31 Universität Tübingen, Germany, 331 pp., 2003.
- 32 Tütken, T., Vennemann, T. W., Janz, H. and Heizmann, E. P. J.: Palaeoenvironment and palaeoclimate  
33 of the Middle Miocene lake in the Steinheim basin, SW Germany: a reconstruction from C, O, and  
34 Sr isotopes of fossil remains, *Palaeogeogr. Palaeoclimatol.*, 241, 457–491, 2006.
- 35 Vellinga, M. and Wood, R. A.: Global climatic impact of a collapse of the Atlantic thermohaline  
36 circulation, *Climatic Changes*, 54, 251–267, 2002.

- 1 Vennemann, T. W., Fricke, H. C., Blake, R. E., Neil, J. R. O. and Colman, A.: Oxygen isotope  
2 analysis of phosphates: a comparison of techniques for analysis of  $\text{Ag}_3\text{PO}_4$ , *Chem. Geol.*, 185, 321–  
3 336, 2002.
- 4 Waller, T. R.: Scanning electron microscopy of shell and mantle in the order Arcoida (Mollusca:  
5 Bivalvia), *Smithsonian Contributions to Zoology*, 313, 1–58, 1980.
- 6 Wanamaker, A. D., Kreutz, K. J., Schöne, B. R. and Introne, D. S.: Gulf of Maine shells reveal  
7 changes in seawater temperature seasonality during the edieval limate nomaly and the Little Ice Age,  
8 *Palaeogeogr. Palaeocl.*, 302, 43–51, 2011.
- 9 Zachos, J. C., Dickens, G. R. and Zeebe, R. E.: An early Cenozoic perspective on greenhouse warming  
10 and carbon-cycle dynamics., *Nature*, 451, 279–283, 2008.

11

## 1 **Figure Captions**

2 Figure 1. Map showing the paleogeography during the Rupelian stage and the sample locality  
3 in the Mainz Basin. (A) Position of the Mainz Basin (MB) in Central Europe. URG = Upper  
4 Rhine Graben. Emerged land areas are shown in brown and marine environments in blue.  
5 Modified from Spiegel et al. (2007). (B) Sample locality of the shells (outcrop ‘Trift’ near  
6 Weinheim; white dot) and sea cow teeth (red dots). The presence of a western gateway  
7 (dashed area) connecting the Mainz Basin to the Paris Basin is unclear. Dashed line denotes  
8 the tectonic boundary between the MB and URG. Modified after Grimm et al. (2011). (C)  
9 Photograph of the outcrop “Trift” near Weinheim, type locality of the Alzey Formation from  
10 which the bivalves were collected.

11

12 Figure 2. Macroscopic and microscopic views of the studied shell material (*Glycymeris*  
13 *planicostalis*) from the early Oligocene of the Mainz Basin. (A) Left valve. Dotted lines =  
14 cutting axis. (B) Outer and inner portions of the outer shell layer (oOSL, iOSL) as well as the  
15 inner shell layer (ISL) are clearly visible in the umbo-ventral margin cross-section (dotted line  
16 in A) of specimen EOW-MB-Wht-7. (C) Carbonate powder was collected from the outer shell  
17 layer after removing the outer chalky shell portions. Arrows point to annual growth lines. (D-  
18 G) SEM images show the extraordinary preservation state of the studied shell material.  
19 Primary microstructures are still present. (D) Outer crossed-lamellar layer, (E) inner complex  
20 crossed-lamellar layer and (F) transition zone between outer and inner shell layer (dotted  
21 lines). Arrows point to tubule openings. (G) Detailed view of a tubule. The lack of diagenetic  
22 fillings inside the cavity further supports the absence of any significant diagenetic overprint.  
23 (H) Distinct growth lines (yellow dotted lines) are visible in the hinge plate of Mutvei-stained  
24 cross-sections. DOG=direction of growth.

1

2 Figure 3. Cross-plot of mammal tooth enamel  $\delta^{18}\text{O}_{\text{PO}_4}$  and  $\delta^{18}\text{O}_{\text{CO}_3}$  pairs (dashed line =  
3 average; grey area = 95% prediction intervals) compiled by Pellegrini et al. (2011) with  
4 respective data from the seven Oligocene sirenian teeth of the present study (red filled  
5 circles). Sea cow isotope data plot within the 95% prediction intervals suggesting that  
6 diagenesis has not affected the isotope composition of the phosphate group.

7

8 Figure 4. Raw (grey) and re-sampled (black)  $\delta^{18}\text{O}_{\text{shell}}$  values for each of the three *Glycymeris*  
9 *planicostalis* shells analyzed in this study (A = MB-Wht-2; B = MB-Wht-4; C = MB-Wht-7).  
10 Vertical dotted bars represent annual growth lines. Temperatures were calculated using Eq. 2  
11 with a  $\delta^{18}\text{O}_{\text{water}}$  value reconstructed from  $\delta^{18}\text{O}_{\text{PO}_4}$  values of sea cow tooth enamel (see text for  
12 description).

13

14 Figure 5. Average seasonal temperature changes (black dots,  $\pm 1\sigma$ ) based on mathematically  
15 re-sampled shell oxygen isotope values ( $\delta^{18}\text{O}_{\text{shell}}$  values; see text for explanation) of 40  
16 annual increments measured in three specimens of *Glycymeris planicostalis*. Note that the  
17 resultant temperature curve is not symmetric as one would expect, but right-skewed indicating  
18 slower shell growth occurred during fall and winter than during the remainder of the year. In  
19 other words, more shell material has been deposited during spring and summer than during  
20 fall and winter.

21

22 Figure 6. Seasonal temperature ranges. (A) Comparison between raw (circles) and  
23 mathematically re-sampled (squares) summer (red) and winter (blue) temperature data based

1 on shell oxygen isotope data of three fossil *Glycymeris planicostalis* shells. Whereas  
2 mathematical re-sampling did not greatly affect average values and winter ranges, the summer  
3 temperature range of re-sampled data is truncated. (B) Comparison of the reconstructed  
4 temperature data based on  $\delta^{18}\text{O}_{\text{shell}}$  values of the three studied bivalve shells (filled black  
5 circle) and previously published temperature data based on planktonic foraminifera (Grimm,  
6 1994), shark teeth (Tütken, 2003) and palynological associations (Pross et al., 2000). (C)  
7 Seawater temperatures off Lebanon and southern France at 35 m depth (Abboud-Abi Saab et  
8 al., 2004) and air temperatures in southern France (GHCN Monthly Dataset; Lawrimore et al.,  
9 2011).

10

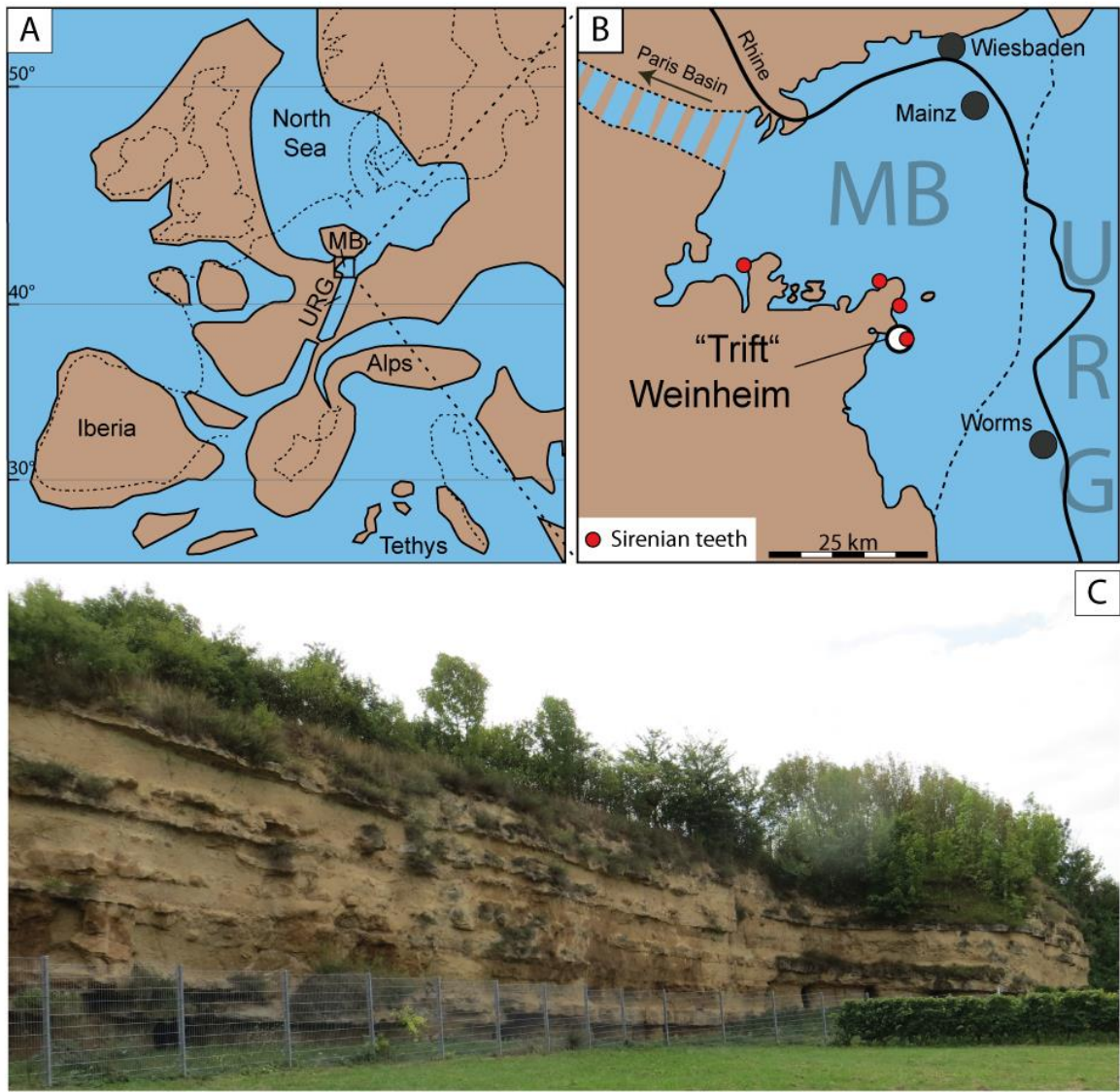
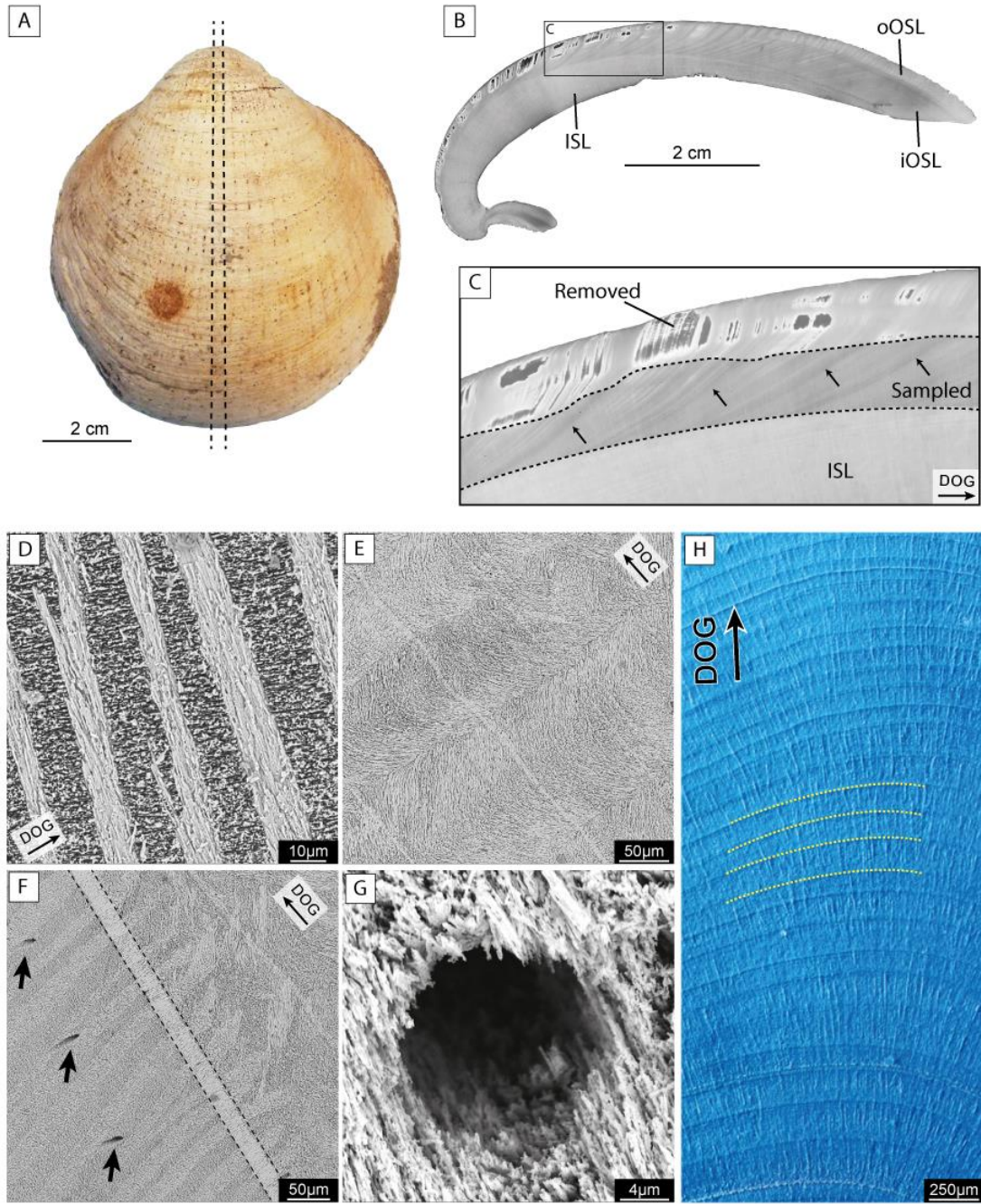
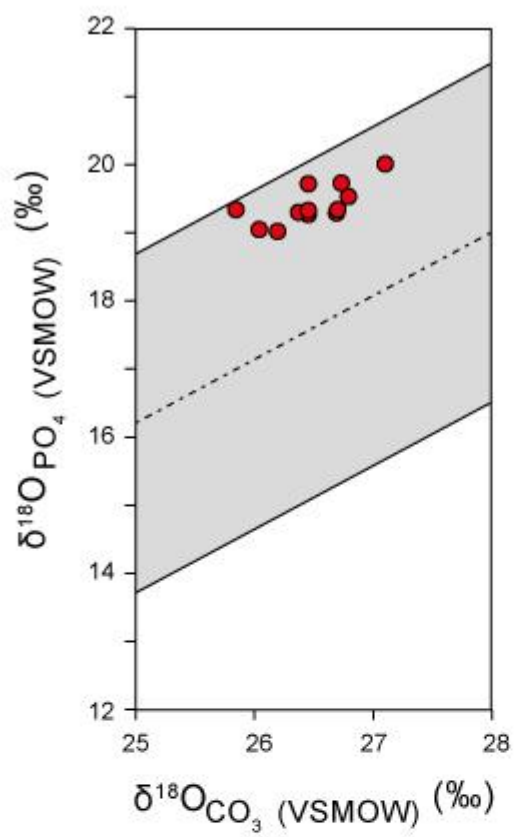


Figure 1

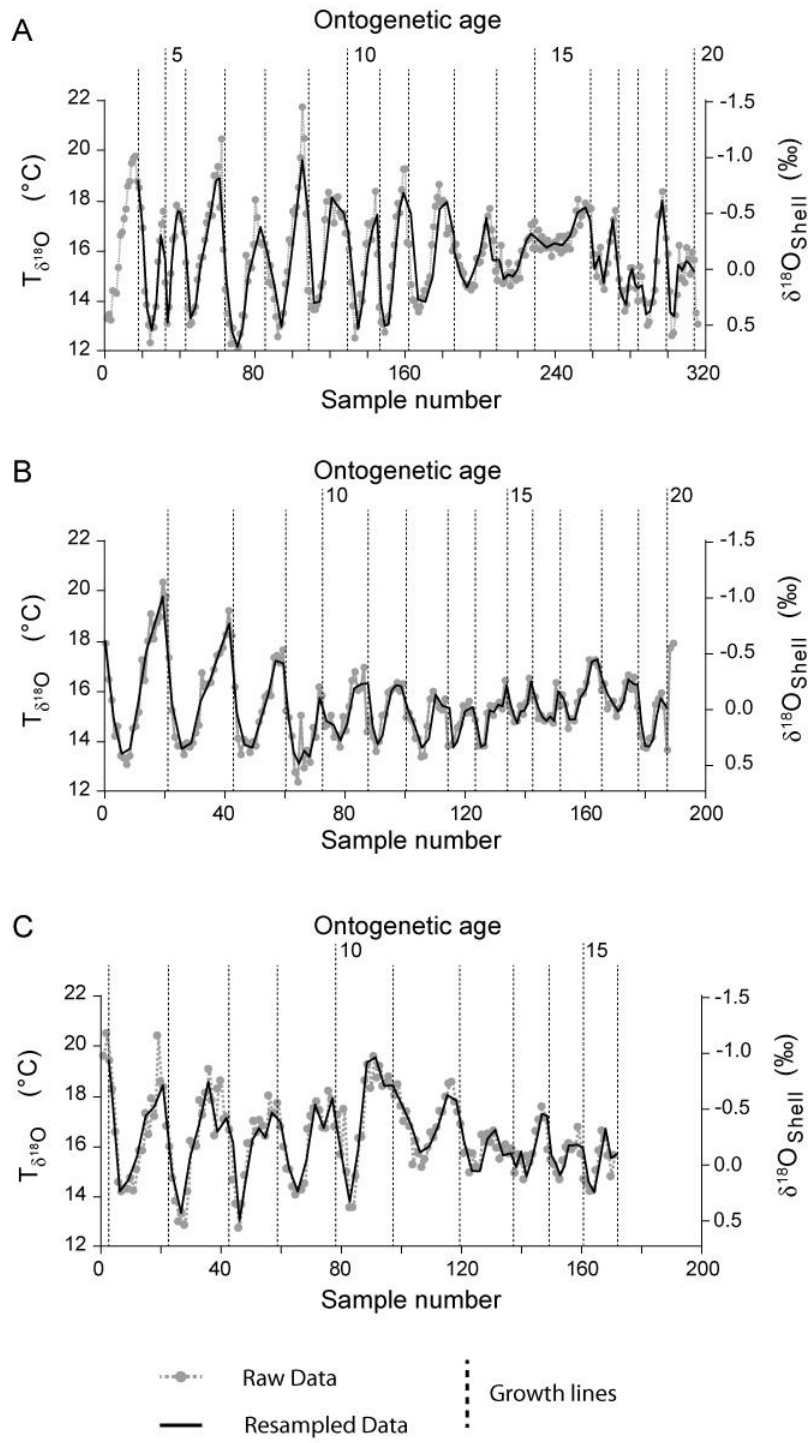




**Figure 2**



**Figure 3**



1

Figure 4

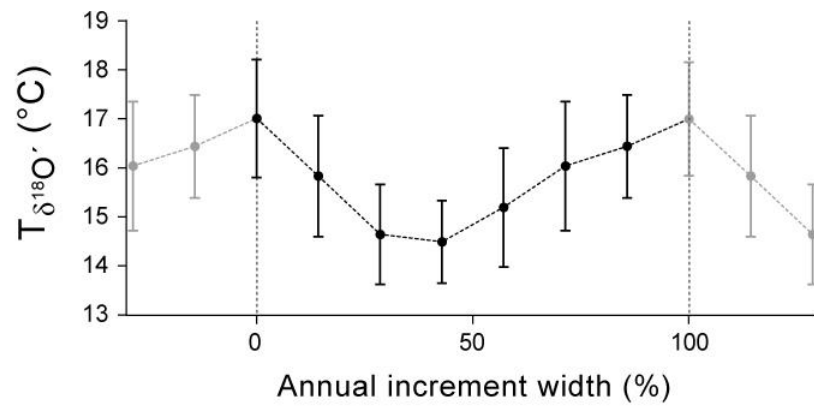


**Figure 5**

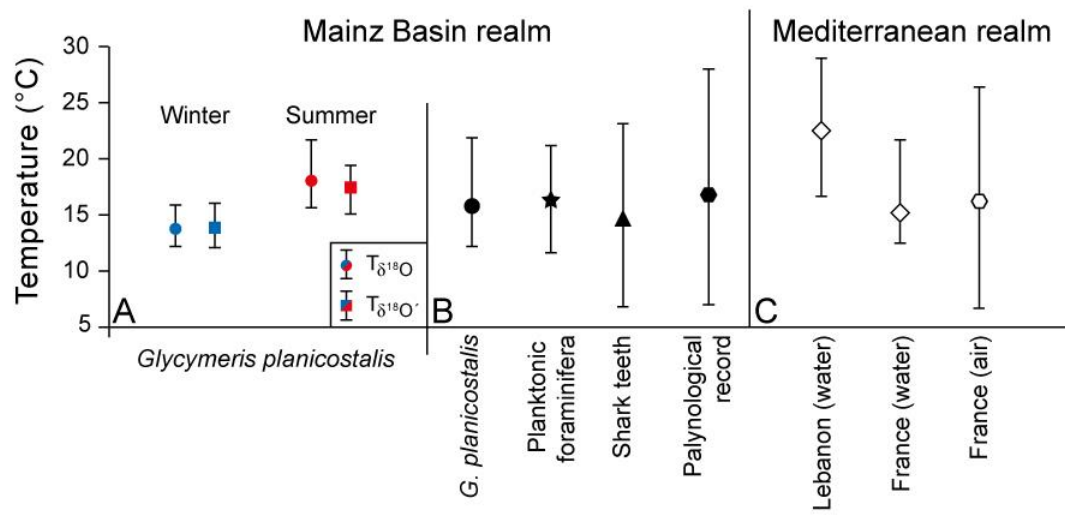


**Figure 6**

1 **Table Captions**

2 Table 1. Enamel  $\delta^{18}\text{O}_{\text{PO}_4}$  and  $\delta^{18}\text{O}_{\text{CO}_3}$  values (VSMOW) of the sea cow teeth from the Alzey  
 3 Formation deposits of the Mainz Basin and  $\delta^{18}\text{O}_{\text{water}}$  values calculated from the sea cow  
 4 enamel  $\delta^{18}\text{O}_{\text{PO}_4}$  values. See text for details.

Sample ID	Sample Locality	$\delta^{18}\text{O}_{\text{PO}_4}$ [‰]	$\delta^{18}\text{O}_{\text{CO}_3}$ [‰]	$\delta^{18}\text{O}_{\text{water}}$ [‰]
Trai 01-1	Traisen	19.36	25.79	-1.01
Trai 01-2	Traisen	19.04	26.14	-1.38
Eck 01-1	Eckelsheim	19.29	26.40	-1.09
Eck 01-2	Eckelsheim	19.74	26.40	-0.57
Wein 01-1	Weinheim	19.31	26.63	-1.07
Wein 01-2	Weinheim	19.36	26.64	-1.01
PW 2008/5017-LS-2-1	Alzey- Weinheim	19.32	26.31	-1.06
PW 2008/5017-LS-2-2	Alzey- Weinheim	19.55	26.74	-0.79
PW 2008/5017-LS-1B	Alzey- Weinheim	20.03	27.05	-0.23
PW 2008/5017-LS-1A	Alzey- Weinheim	19.35	26.40	-1.02
STS-BE 62-1	Eckelsheim	19.07	25.98	-1.35
PW 2005/5042-LS-1	Wendelsheim	19.75	26.67	-0.56
Average $\pm 1\sigma$		19.43 $\pm$ 0.29	26.43 $\pm$ 0.35	-0.9 $\pm$ 0.3
Min		19.04	25.79	-1.38
Max		20.03	27.05	-0.23

1 Table 2. Oxygen isotope values ( $\delta^{18}\text{O}$  vs. VPDB) of the three *Glycymeris planicostalis* shells  
 2 analyzed in this study. The table lists seasonal extremes ( $\delta^{18}\text{O}_{\text{min}}$  and  $\delta^{18}\text{O}_{\text{max}}$ ) as well as  
 3 average summer ( $\delta^{18}\text{O}'_{\text{summer}}$ ; re-sampled values; explanation see text) and winter extremes  
 4 values ( $\delta^{18}\text{O}'_{\text{winter}}$ ).

---

Sample ID	$\delta^{18}\text{O}_{\text{min}}$ [‰]	$\delta^{18}\text{O}'_{\text{summer}} \pm 1\sigma$ [‰]	$\delta^{18}\text{O}_{\text{max}}$ [‰]	$\delta^{18}\text{O}'_{\text{winter}} \pm 1\sigma$ [‰]	$\delta^{18}\text{O}_{\text{mean}} \pm 1\sigma$ [‰]
MB-Wht-2	-1.48	$-0.66 \pm 0.21$	0.75	$0.38 \pm 0.23$	$-0.12 \pm 0.13$
MB-Wht-4	-1.16	$-0.40 \pm 0.31$	0.67	$0.28 \pm 0.14$	$-0.03 \pm 0.13$
MB-Wht-7	-1.19	$-0.61 \pm 0.23$	0.60	$0.24 \pm 0.19$	$-0.20 \pm 0.16$

---

5

6

7

1 Table 3. Dentine and enamel  $\delta^{18}\text{O}_{\text{PO}_4}$  values (VSMOW) of shark teeth recovered from the  
 2 early Oligocene deposits of the Mainz Basin (Tütken, 2003). Values have been converted to  
 3 temperature ( $T\delta^{18}\text{O}_{\text{PO}_4}$ ) using the paleothermometry equation by Longinelli and Nutti (1973)  
 4 assuming  $\delta^{18}\text{O}_{\text{water}} = -0.9\text{‰}$ .

5

Sample ID	Genus	$\delta^{18}\text{O}_{\text{PO}_4}$ [‰]	$T\delta^{18}\text{O}_{\text{PO}_4}$ [°C]
FD HAI MB 2	<i>Carcharias</i> sp.	22.9	9.1
FZ HAI MB 2	<i>Carcharias</i> sp.	22.8	9.5
FZ HAI MB 3	<i>Carcharias</i> sp.	19.6	23.3
FD HAI MB 4	<i>Carcharias</i> sp.	21.0	17.2
FZ HAI MB 4	<i>Carcharias</i> sp.	21.5	15.1
FZ HAI MB 8	<i>Carcharias</i> sp.	20.1	21.1
FZ HAI MB 9	<i>Carcharias</i> sp.	21.0	17.2
FZ HAI MB 10	<i>Carcharias</i> sp.	23.4	6.9
Average $\pm 1\sigma$		$21.5 \pm 1.3$	$14.9 \pm 5.9$
Min		19.6	6.9
Max		23.4	23.3

6

7

8



1 Table 4. Oxygen isotope values ( $\delta^{18}\text{O}$  vs. VPDB) of foraminiferan tests from the Bodenheim  
 2 Formation (wells Kriegsfeld 5 and Bodenheim 65) reported by Grimm (1994).  $\delta^{18}\text{O}_{\text{Glob}}$  =  
 3 *Globigerina* sp. (planktonic foraminifera);  $\delta^{18}\text{O}_{\text{Bol}}$  = *Bolivina* sp. (benthonic foraminifera).  
 4 Values have been converted to temperature ( $T\delta^{18}\text{O}_{\text{Glob}}$ ,  $T\delta^{18}\text{O}_{\text{Bol}}$ ) using the equation by  
 5 Anderson and Arthur (1983) assuming  $\delta^{18}\text{O}_{\text{w}} = -0.9\text{‰}$ .

Kriegsfeld 5			Bodenheim 65		
Depth [m]	$\delta^{18}\text{O}_{\text{Glob}}$ [‰]	$T\delta^{18}\text{O}_{\text{Glob}}$ [°C]	Depth [m]	$\delta^{18}\text{O}_{\text{Bol}}$ [‰]	$T\delta^{18}\text{O}_{\text{Bol}}$ [°C]
15	-1.8	18.7	21.5	1.5	5.9
23	-2.4	21.3	70	-0.9	14.9
25	-0.1	11.7	80	1.0	7.6
28	-1.3	16.5	85	1.1	7.3
30	-2.0	19.5	90	0.7	8.7
32	-0.7	14.1	95	-0.03	11.4
34	-0.8	14.5	99	0.7	8.7
Average $\pm 1\sigma$	$2.75 \pm 0.81$	$16.6 \pm 3.4$	Average	$0.6 \pm 0.8$	$9.5 \pm 2.9$
Min	-2.4	11.7	Min	-0.9	5.9
Max	-0.1	21.3	Max	1.5	14.9

6

7

8